Composite Structures 256 (2021) 113028

Contents lists available at ScienceDirect

Composite Structures

journal homepage: www.elsevier.com/locate/compstruct

Vibrations of double-nanorod-systems with defects using nonlocal-integral-surface energy-based formulations

Keivan Kiani [a,1], Krzysztof Kamil Żur [b,*]

[a] Department of Civil Engineering, K.N. Toosi University of Technology, Valiasr Ave., P.O. Box 15875-4416 Tehran, Iran
[b] Faculty of Mechanical Engineering, Bialystok University of Technology, Wiejska 45C Street, 15-351 Bialystok, Poland

ARTICLE INFO

Keywords:
Vibration
Doubly defected nanorods
Galerkin method
Admissible modes
Nonlocal-integral elasticity theory
Surface elasticity theory

ABSTRACT

We report suitable surface energy-nonlocal-integral and -differential models for investigating mechanical behavior of a nanosystem consists of double parallel nanorods with defects. By visualizing the locally caused defects by appropriate linear springs, the equations of motion that display longitudinal vibrations of the defected nanosystem are derived accounting for nonlocality and surface energy effects. For the nanosystem at hand with a single defect in each nanorod, there would exist four coupled-integro-partial differential equations with eight boundary conditions. By evaluating the exact nonlocal-surface energy-based modes associated with fixed–fixed and fixed-free defected nanorods according to the nonlocal-differential-based model, Galerkin method is implemented to assess the longitudinal frequencies. The capabilities of the nonlocal-integral-based model in capturing the natural frequencies of the nonlocal-differential-based model for the defected nanosystem with fixed–fixed and fixed-free ends are revealed. The roles of the nonlocality, surface energy, nanorod diameter and length, location and mechanical constants of defects as well as the constant of the elastic interface layer on the free vibration are explained.

1. Introduction

Nanorods are one-dimensional nanostructures of length up to one-hundred nanometers, which are commonly synthesized from metals and semiconducting materials. They have many potential applications in display technology [1,2], micro-/nano-electromechanical systems [3,4], light-emitting diodes [5,6], and nanosensors [7,8]. Most of these great applications are indebted to the perfect structure of nanorods; nevertheless, defects can be inevitably produced in nanorods due to the vacancies and dislocations during the synthesis process as well as externally applied loads. Commonly, the defects endanger the anticipated duties of nanorods, particularly their crucial tasks in bearing the exerted statics and dynamical loads. To optimize the mechanical performance of defected nanorods, the influence of defects on their free dynamic response should be appropriately elucidated.

At the nanoscale level, vibration of each atom is commonly affected by the dynamical motion of its nearby atoms because of inter-atoms bonds. From structural mechanics points of view, it means that the status of stress at each point of the continuum does not only depend on the stress at that point, but also on the status of the stress of its neighboring points (i.e., *nonlocality of stress field*). Such a reality could not be predicted by the classical theory of elasticity (CTE) since it is fundamentally established based on the dependency of the stress field at each point to the stress at that point only. To eliminate such a drawback of the CTE for low-dimensional structures, several advanced continuum theories were developed by investigators over the preceding century. One of the most common theories, which can be applicable to any physical field, is the nonlocal theory of elasticity (NTE) of Eringen [9–12]. In the context of this theory, the nonlocal stress is expressed as the integral of the product of a kernel function and the local stress (i.e., classical stress) over the spatial domain of the structure. The kernel function is an attenuating function with a compact support domain whose coefficient is determined such that the integral of the kernel function over the volume of the structure would be equal to one. The kernel function at each point relies on the point's distance from the point whose stress is of concern as well as the length-scale. The length-scale or small-scale parameter for each material is generally a function of its atomic bond length. Commonly, the value of this factor is calculated such that leads to the best correspondence between

* Corresponding author.
E-mail addresses: kiani@kntu.ac.ir, keivankiani@yahoo.com (K. Kiani), k.zur@pb.edu.pl (K.K. Żur).
[1] Dedicated to the honorable memory of my beloved mother, Kobra Ahmadi (1950–July 21, 2020).

https://doi.org/10.1016/j.compstruct.2020.113028
Received 2 July 2020; Revised 19 September 2020; Accepted 23 September 2020
Available online 30 September 2020

the predicted dispersion curves by the nonlocal model and those of a suitable atomic methodology like molecular dynamics, density-functional theory, and so on. Up to now, the NTE of Eringen has been frequently employed for mechanical analysis of various structures at the nanoscale, including nanorods [13–19], nanobeams [20–36], and nanoplates [37–42]; however, application of differential-based formulations of the NTE to the problems of cantilevered nanobeams leads to some paradoxical mechanical response [43–45]. In recent years, nonlocal-strain gradient-based models have been also applied to the buckling and vibrational problems of beam-like and plate-like nanostructures [46–49]. By this brief literature review, herein, both nonlocal-differential and nonlocal-integral formulations for axial vibration analysis of the defected nanosystem are presented.

The dynamical analysis of individual nanorods using the NTE has been focus of attention of investigators in the past decade [50–59]. Additionally, longitudinal vibration of and wave propagation in nanosystems consist of double or multiple elastic (viscoelastic) nanorods [60–63] have been examined by employing the NTE, and an inclusive knowledge regarding the influence of the nonlocality on their free dynamics response is now available; however, the mechanical behavior of defected nanorod systems have not been displayed yet.

By decreasing the dimensions of structures, the ratio of the surface area to the volume generally increases. It implies that if a low-dimensional structure could be somehow decomposed into the surface and the bulk, the share of kinetic and strain energy of the surface in the total energy would not be negligible anymore. Based on this original idea, Gurtin and Morduch [64–67] proposed the surface theory of elasticity (STE) of solids. In such a context, the surface is a very thin layer with an infinitesimal thickness that has been strongly attached to the bulk. The material constants of the surface layer, namely residual stress in unrestrained condition as well as the Lamé constants, are commonly determined by comparing the predicted results by the STE and those of another atomic-based approach. The STE by Gurtin and Murdoch has been widely employed for capturing the mechanical response of nanorods, nanobeams, and nanoplates [68–77].

To take into account both surface energy and nonlocality in modeling of nanorods, a wise choice is to use a nonlocal-surface energy-based theory (NSTE). In this regard, Kiani [78] examined nonlocal-surface energy-based axial vibrations of an elastically supported nanorod. To this end, nonlocal-integral equations of motion of the nanostructure were derived, and then solved via a meshless technique as well as modal analysis for natural axial frequencies. In contrast to the differential-based models in which nonlocality was incorporated into the mass and deriving forces, in the newly established model, the nonlocality was exclusively incorporated into the stiffness term, indicating a more reasonable and engineering sense. In another work, Kiani [79] investigated longitudinal vibration of functionally graded nanorods with varying cross-section. The problem was formulated in the context of the NSTE through developing nonlocal-integro equations, and then solved by the RKPM and Galerkin approach through employing admissible modes associated with fixed–fixed and fixed-free end conditions.

Despite many conducted scientific works on vibrations of individual nanorods as well as multiple-nanorod-systems, the influence of defects on their vibrations has been rarely investigated. In this regard, Hsu et al. [80] analytically studied nonlocal axial frequencies of clamped–clamped and clamped-free nanorods with a single cracked zone. The existence of the crack was introduced to the model via an axial spring at the location of the occurrence of the crack. The influences of the crack parameters (intensity and location) as well as the nonlocal parameter on the fundamental frequency of the cracked nanostructure was explained. Yayli and Cercevik [81] established an analytical nonlocal elasticity-based model to examine axial vibration of cracked nanorods and carbon nanotubes with arbitrary boundary conditions. Through modeling of the fractured zone by an axial spring, the axial displacement was appropriately expressed by using Fourier's series accounting for the axial stiffness of ends' springs. Additionally, flexural and torsional vibrations of cracked nanorods and nanobeams have been of interest of some scholars during recent years [82–84].

This brief literature survey clearly reveals that the longitudinal free dynamic response of locally defected double-nanorod-systems has not been considered yet. To bridge this scientific gap, herein we are interested in exclusive exploring free vibration behavior of double-nanorod-systems with local defects through developing suitable nonlocal-differential and nonlocal-integral models. Using the STE of Gurtin and Murdoch, the equations of motion are presented according to both nonlocal-differential and nonlocal-integral continuum-based theory of Eringen. To this end, the locally caused defects and the dynamic interactions of double nanorods have been modeled by linear springs and an elastic interface layer, respectively. The resulting coupled integro-partial differential equations are then solved by using Galerkin-based admissible mode method. For most common boundary conditions (i.e., fixed-free and fixed–fixed), the influences of crucial factors on the natural frequencies are investigated. The capabilities of the nonlocal-differential model in capturing the frequencies of the nonlocal-integral model are presented for particular cases. Special attention is also paid to the effects of nonlocality and surface energy on the dynamical response of the nanosystem. The achieved results from this comprehensive study and the suggested approach provide very helpful insights for dynamic analysis of more complex nanosystems consisting of multiple-defected nanorods.

2. Development of a nonlocal-differential-based mathematical model

2.1. Nonlocal-differential-surface energy-based governing equations

Consider a nanosystem consists of doubly parallel nanorods with local defects, as shown in Fig. 1(a). The length and diameter of each circular cylindrical nanorod are denoted by l_b and D_0, respectively. It is assumed that the length of defects is fairly negligible compared to the length of nanorods (i.e., $\Delta c_1, \Delta c_2 \ll l_b$). The distances of the locally defected zones in the first and the second nanorods from the left end in order are denoted by c_1 and c_2. The density, elastic Young's modulus, and cross-sectional area of the bulk of nanorods are represented by ρ_b, E_b, and A_b, respectively, while those of the surface in order are ρ_0, E_0, and A_0. Essentially, the constitutive nanorods of the nanosystem could interact with each other due to existing van der Waals (vdW) and interfacial frictional forces. The inter-rod frictional force is ignored in the continuing since the nanosystem's undamped frequencies are of particular concern. Further, the vdW forces between the nanorods' constitutive atoms are assumed to be visualized by an interfacial elastic layer of constant K_L. Let us model the existing local defects within the first and the second nanorods by linear axial springs of constants k_1 and k_2, respectively. From now on, these are called defect factors. Actually, the locally caused defects are assumed to be axisymmetric, otherwise, the longitudinal and transverse vibrations of the nanorods would be coupled with each other, and therefore, the resulting problem would be more complicated than that which is going to be studied in this work. By virtue of all made assumptions, the presented nanosystem in Fig. 1(a) could be now reduced to that demonstrated in Fig. 1(b).

By denoting the longitudinal displacement fields associated with the left and right sides of the defect of the ith nanorod (i.e., its constitutive segments) by $u_i^L = u_i^L(x,t)$ and $u_i^R = u_i^R(x,t)$, respectively, the kinetic energy of the nanosystem accounting for the inertia of the surface layer is written as:

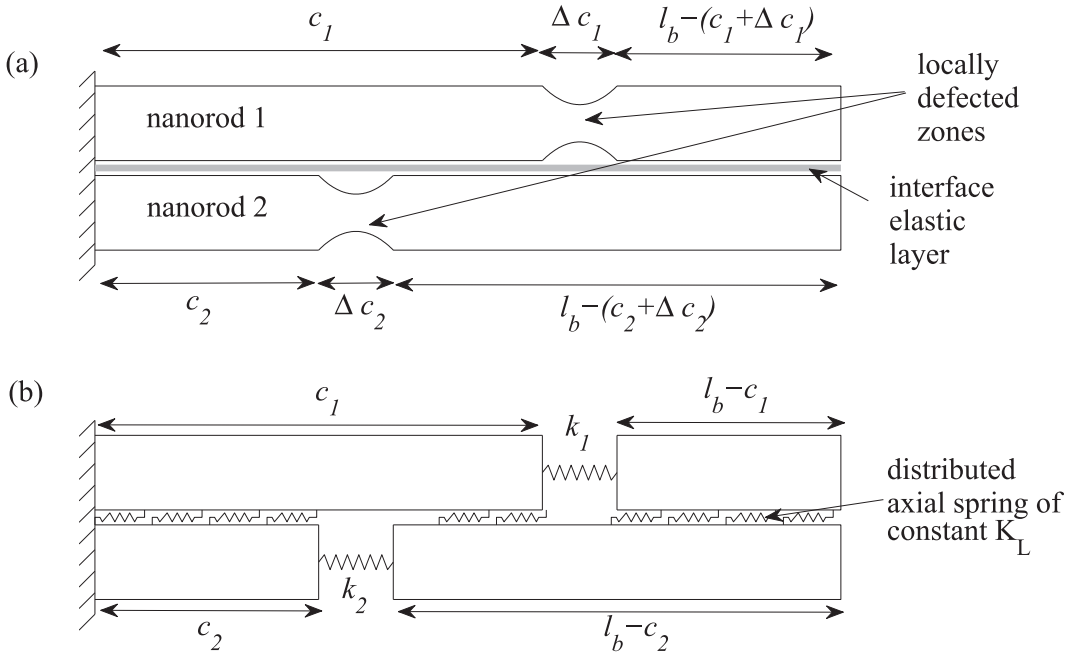

Fig. 1. (a) Schematic representation of a fixed-free double-nanorod-system with local defects; (b) a continuum-based representation of the locally defected nanosystem.

$$T(t)=\tfrac{1}{2}(\rho_0A_0+\rho_bA_b)\sum_{i=1}^{2}\left[\int_0^{c_i}\left(\frac{\partial u_i^L}{\partial t}\right)^2\mathrm{d}x+\int_{c_i}^{l_b}\left(\frac{\partial u_i^R}{\partial t}\right)^2\mathrm{d}x\right], \tag{1}$$

where t is the time parameter.

The elastic strain energy of the nanosystem consists of doubly defected nanorods by considering nonlocality, surface effect, and longitudinally dynamic interaction for the case of $c_1 \geqslant c_2$ is expressed by:

$$\begin{aligned}U(t)=&\tfrac{1}{2}\sum_{i=1}^{2}\left[\int_0^{c_i}N_i^{nl}\left(\frac{\partial u_i^L}{\partial x}\right)\mathrm{d}x+\int_{c_i}^{l_b}N_i^{nl}\left(\frac{\partial u_i^R}{\partial x}\right)\mathrm{d}x\right]\\&+\tfrac{1}{2}\int_0^{c_2}K_L\left(u_1^L-u_2^L\right)^2\mathrm{d}x+\tfrac{1}{2}\int_{c_2}^{c_1}K_L\left(u_1^L-u_2^R\right)^2\mathrm{d}x\\&+\tfrac{1}{2}\int_{c_1}^{l_b}K_L\left(u_2^R-u_2^R\right)^2\mathrm{d}x+\tfrac{1}{2}\sum_{i=1}^{2}k_i\left(u_i^L(c_i,t)-u_i^R(c_i,t)\right)^2,\end{aligned} \tag{2}$$

and in the case of $c_1 \leqslant c_2$, it is modified to:

$$\begin{aligned}U(t)=&\tfrac{1}{2}\sum_{i=1}^{2}\left[\int_0^{c_i}N_i^{nl}\left(\frac{\partial u_i^L}{\partial x}\right)\mathrm{d}x+\int_{c_i}^{l_b}N_i^{nl}\left(\frac{\partial u_i^R}{\partial x}\right)\mathrm{d}x\right]\\&+\tfrac{1}{2}\int_0^{c_1}K_L\left(u_1^L-u_2^L\right)^2\mathrm{d}x+\tfrac{1}{2}\int_{c_1}^{c_2}K_L\left(u_1^R-u_2^L\right)^2\mathrm{d}x\\&+\tfrac{1}{2}\int_{c_2}^{l_b}K_L\left(u_2^R-u_2^R\right)^2\mathrm{d}x+\tfrac{1}{2}\sum_{i=1}^{2}k_i\left(u_i^L(c_i,t)-u_i^R(c_i,t)\right)^2,\end{aligned} \tag{3}$$

where the nonlocal-surface energy-based axial force within the ith nanorod (N_i^{nl}) in the differential form is governed by [78,79]:

$$N_i^{nl}-(e_0a)^2\frac{\partial^2N_i^{nl}}{\partial x^2}=(E_0A_0+E_bA_b)\frac{\partial u_i^{\alpha}}{\partial x}+\tau_0A_0;\quad \alpha=L\text{or}R, \tag{4}$$

in which e_0a is the nonlocal parameter, and τ_0 is the initial stress within the surface under unconstrained condition. By using Hamilton's principle, $\int_0^t(\delta T(t)-\delta U(t))\,\mathrm{d}t=0$, where δ is the variational symbol, the equations of motion of the nanosystem with local defects accounting for nonlocality and surface energy effect are obtained as follows for the case of $c_1 \geqslant c_2$:

$$\begin{aligned}&(\rho_bA_b+\rho_0A_0)\left(\frac{\partial^2u_1^L}{\partial t^2}-(e_0a)^2\frac{\partial^4u_1^L}{\partial t^2\partial x^2}\right)-(E_bA_b+E_0A_0)\frac{\partial^2u_1^L}{\partial x^2}\\&+K_L\left(\left(u_1^L-u_2^L\right)-(e_0a)^2\left(\frac{\partial^2u_1^L}{\partial x^2}-\frac{\partial^2u_2^L}{\partial x^2}\right)\right)\mathrm{H}(c_2-x)+K_L\\&\times\left(\left(u_1^L-u_2^R\right)-(e_0a)^2\left(\frac{\partial^2u_1^L}{\partial x^2}-\frac{\partial^2u_2^R}{\partial x^2}\right)\right)(\mathrm{H}(c_1-x)-\mathrm{H}(c_2-x))=0;\ 0<x<c_1,\end{aligned} \tag{5a}$$

$$\begin{aligned}&(\rho_0A_0+\rho_0A_0)\left(\frac{\partial^2u_1^R}{\partial t^2}-(e_0a)^2\frac{\partial^4u_1^R}{\partial t^2\partial x^2}\right)-(E_bA_b+E_0A_0)\frac{\partial^2u_1^R}{\partial x^2}\\&+K_L\left(\left(u_1^R-u_2^R\right)-(e_0a)^2\left(\frac{\partial^2u_1^R}{\partial x^2}-\frac{\partial^2u_2^R}{\partial x^2}\right)\right)=0;\ c_1<x<l_b,\end{aligned} \tag{5b}$$

$$\begin{aligned}&(\rho_bA_b+\rho_0A_0)\left(\frac{\partial^2u_2^L}{\partial t^2}-(e_0a)^2\frac{\partial^4u_2^L}{\partial t^2\partial x^2}\right)-(E_bA_b+E_0A_0)\frac{\partial^2u_2^L}{\partial x^2}\\&+K_L\left(\left(u_2^L-u_1^L\right)-(e_0a)^2\left(\frac{\partial^2u_2^L}{\partial x^2}-\frac{\partial^2u_1^R}{\partial x^2}\right)\right)=0;\ 0<x<c_2,\end{aligned} \tag{5c}$$

$$\begin{aligned}&(\rho_bA_b+\rho_0A_0)\left(\frac{\partial^2u_2^R}{\partial t^2}-(e_0a)^2\frac{\partial^4u_2^R}{\partial t^2\partial x^2}\right)-(E_bA_b+E_0A_0)\frac{\partial^2u_2^R}{\partial x^2}\\&+K_L\left(\left(u_2^R-u_1^L\right)-(e_0a)^2\left(\frac{\partial^2u_2^R}{\partial x^2}-\frac{\partial^2u_1^L}{\partial x^2}\right)\right)(\mathrm{H}(c_1-x)-\mathrm{H}(c_2-x))+K_L\\&\times\left(\left(u_2^R-u_1^R\right)-(e_0a)^2\left(\frac{\partial^2u_2^R}{\partial x^2}-\frac{\partial^2u_1^R}{\partial x^2}\right)\right)(1-\mathrm{H}(c_1-x))=0;\ c_2<x<l_b,\end{aligned} \tag{5d}$$

and for the case of $c_1 < c_2$, the nonlocal-surface energy-based equations of the locally defected nanosystem take the following form:

$$\begin{aligned}&(\rho_bA_b+\rho_0A_0)\left(\frac{\partial^2u_1^L}{\partial t^2}-(e_0a)^2\frac{\partial^4u_1^L}{\partial t^2\partial x^2}\right)-(E_bA_b+E_0A_0)\frac{\partial^2u_1^L}{\partial x^2}\\&+K_L\left(\left(u_1^L-u_2^L\right)-(e_0a)^2\left(\frac{\partial^2u_1^L}{\partial x^2}-\frac{\partial^2u_2^R}{\partial x^2}\right)\right)=0;\ 0<x<c_1,\end{aligned} \tag{6a}$$

$$\begin{aligned}&(\rho_bA_b+\rho_0A_0)\left(\frac{\partial^2u_1^R}{\partial t^2}-(e_0a)^2\frac{\partial^4u_1^R}{\partial t^2\partial x^2}\right)-(E_bA_b+E_0A_0)\frac{\partial^2u_1^R}{\partial x^2}\\&+K_L\left(\left(u_1^R-u_2^L\right)-(e_0a)^2\left(\frac{\partial^2u_1^R}{\partial x^2}-\frac{\partial^2u_2^L}{\partial x^2}\right)\right)(\mathrm{H}(c_2-x)-\mathrm{H}(c_1-x))+K_L\\&\times\left(\left(u_1^R-u_2^R\right)-(e_0a)^2\left(\frac{\partial^2u_1^R}{\partial x^2}-\frac{\partial^2u_2^R}{\partial x^2}\right)\right)(1-\mathrm{H}(c_2-x))=0;\ c_1<x<l_b,\end{aligned} \tag{6b}$$

$$\begin{aligned}&(\rho_bA_b+\rho_0A_0)\left(\frac{\partial^2u_2^L}{\partial t^2}-(e_0a)^2\frac{\partial^4u_2^L}{\partial t^2\partial x^2}\right)-(E_bA_b+E_0A_0)\frac{\partial^2u_2^L}{\partial x^2}\\&+K_L\left(\left(u_2^L-u_1^L\right)-(e_0a)^2\left(\frac{\partial^2u_2^L}{\partial x^2}-\frac{\partial^2u_1^L}{\partial x^2}\right)\right)\mathrm{H}(c_1-x)+K_L\\&\times\left(\left(u_2^L-u_1^R\right)-(e_0a)^2\left(\frac{\partial^2u_2^L}{\partial x^2}-\frac{\partial^2u_1^R}{\partial x^2}\right)\right)(\mathrm{H}(c_2-x)-\mathrm{H}(c_1-x))=0;\ 0<x<c_2,\end{aligned} \tag{6c}$$

$$\begin{aligned}&(\rho_0A_0+\rho_0A_0)\left(\frac{\partial^2u_2^R}{\partial t^2}-(e_0a)^2\frac{\partial^4u_2^R}{\partial t^2\partial x^2}\right)-(E_bA_b+E_0A_0)\frac{\partial^2u_2^R}{\partial x^2}\\&+K_L\left(\left(u_2^R-u_1^R\right)-(e_0a)^2\left(\frac{\partial^2u_2^R}{\partial x^2}-\frac{\partial^2u_1^R}{\partial x^2}\right)\right)=0;\ c_2<x<l_b,\end{aligned} \tag{6d}$$

where H denotes the Heaviside step function.

With regard to the continuity of the nonlocal axial force at the location of local defects and through modeling of the defects via massless linear springs, the following nonclassical boundary conditions could be considered at the interface of the constitutive segments of each nanorod:

$$k_1\left[u_1^R(c_1,t)-u_1^L(c_1,t)\right]=\left[(E_bA_b+E_0A_0)+(e_0a)^2(\rho_bA_b+\rho_0A_0)\frac{\partial^2}{\partial t^2}\right]\frac{\partial u_1^L}{\partial x}(c_1,t)+(e_0a)^2K_L\left(\frac{\partial u_1^L}{\partial x}(c_1,t)-\frac{\partial u_2^R}{\partial x}(c_1,t)\right), \tag{7a}$$

$$\frac{\partial}{\partial x}\left\{(E_bA_b+E_0A_0)u_1^L(c_1,t)+(e_0a)^2\left[(\rho_bA_b+\rho_0A_0)\frac{\partial^2u_1^L}{\partial t^2}(c_1,t)+K_L\left(u_1^L(c_1,t)-u_2^R(c_1,t)\right)\right]\right\}=\frac{\partial}{\partial x}\left\{(E_bA_b+E_0A_0)u_1^R(c_1,t)+(e_0a)^2\left[(\rho_bA_b+\rho_0A_0)\frac{\partial^2u_1^R}{\partial t^2}(c_1,t)+K_L\left(u_1^R(c_1,t)-u_2^R(c_1,t)\right)\right]\right\}, \tag{7b}$$

$$k_2\left[u_2^R(c_2,t)-u_2^L(c_2,t)\right]=\left[(E_bA_b+E_0A_0)+(e_0a)^2(\rho_bA_b+\rho_0A_0)\frac{\partial^2}{\partial t^2}\right]\frac{\partial u_2^L}{\partial x}(c_2,t)+(e_0a)^2K_L\left(\frac{\partial u_2^L}{\partial x}(c_2,t)-\frac{\partial u_1^L}{\partial x}(c_2,t)\right), \tag{7c}$$

$$\frac{\partial}{\partial x}\left\{(E_bA_b+E_0A_0)u_2^L(c_2,t)+(e_0a)^2\left[(\rho_bA_b+\rho_0A_0)\frac{\partial^2u_2^L}{\partial t^2}(c_2,t)+K_L\left(u_2^L(c_2,t)-u_1^L(c_2,t)\right)\right]\right\}=\frac{\partial}{\partial x}\left\{(E_bA_b+E_0A_0)u_2^R(c_2,t)+(e_0a)^2\left[(\rho_bA_b+\rho_0A_0)\frac{\partial^2u_2^R}{\partial t^2}(c_2,t)+K_L\left(u_2^R(c_2,t)-u_1^L(c_2,t)\right)\right]\right\}. \tag{7d}$$

Eqs. (7b) and (7d) display the continuity of the nonlocal axial force of the segments close to the consisting local defects. Furthermore, Eqs. (7a) and (7c) relate the axial rigidity of the axisymmetric defects to the nonlocal axial force in its nearby segments in the linear form. Also, it should be noticed that the term τ_0A_0 has not been included in Eqs. (7a) and (7c) since this results in static axial deformation within the nanosystem which is not of our concern. For more systematic frequency analyzing of the problem, we consider the following dimensionless quantities:

$$\xi=\frac{x}{l_b},\quad \bar{u}_i^a=\frac{u_i^a}{l_b},\quad \bar{c}_i=\frac{c_i}{l_b},\quad \mu=\frac{e_0a}{l_b},\quad \tau=\frac{t}{l_b}\sqrt{\frac{E_b}{\rho_b}},\quad \bar{k}_i=\frac{k_il_b}{E_bA_b},\quad \overline{K}_L=\frac{K_Ll_b^2}{E_bA_b},\quad \chi_1^2=\frac{\rho_0A_0}{\rho_bA_b},\quad \chi_2^2=\frac{E_0A_0}{E_bA_b}. \tag{8}$$

By introducing Eq. (8) to Eqs. (5a)-(5d) as well as Eqs. (6a)-(6d), the dimensionless-nonlocal-surface energy-based equations of motion of the defected nanosystem in the case of $\bar{c}_1\geqslant\bar{c}_2$ take the following form:

$$\begin{aligned}&(1+\chi_1^2)\left(\frac{\partial^2\bar{u}_1^L}{\partial\tau^2}-\mu^2\frac{\partial^4\bar{u}_1^L}{\partial\tau^2\partial\xi^2}\right)-(1+\chi_2^2)\frac{\partial^2\bar{u}_1^L}{\partial\xi^2}\\&+\overline{K}_L\left((\bar{u}_1^L-\bar{u}_2^L)-\mu^2\left(\frac{\partial^2\bar{u}_1^L}{\partial\xi^2}-\frac{\partial^2\bar{u}_2^L}{\partial\xi^2}\right)\right)\mathrm{H}(\bar{c}_2-\xi)+\overline{K}_L\\&\times\left((\bar{u}_1^L-\bar{u}_2^R)-\mu^2\left(\frac{\partial^2\bar{u}_1^L}{\partial\xi^2}-\frac{\partial^2\bar{u}_2^R}{\partial\xi^2}\right)\right)(\mathrm{H}(\bar{c}_1-\xi)-\mathrm{H}(\bar{c}_2-\xi))=0;\quad 0<\xi<\bar{c}_1,\end{aligned} \tag{9a}$$

$$\begin{aligned}&(1+\chi_1^2)\left(\frac{\partial^2\bar{u}_1^R}{\partial\tau^2}-\mu^2\frac{\partial^4\bar{u}_1^R}{\partial\tau^2\partial\xi^2}\right)-(1+\chi_2^2)\frac{\partial^2\bar{u}_1^R}{\partial\xi^2}\\&+\overline{K}_L\left((\bar{u}_1^R-\bar{u}_2^R)-\mu^2\left(\frac{\partial^2\bar{u}_1^R}{\partial\xi^2}-\frac{\partial^2\bar{u}_2^R}{\partial\xi^2}\right)\right)=0;\ \bar{c}_1<\xi<1,\end{aligned} \tag{9b}$$

$$\begin{aligned}&(1+\chi_1^2)\left(\frac{\partial^2\bar{u}_2^L}{\partial\tau^2}-\mu^2\frac{\partial^4\bar{u}_2^L}{\partial\tau^2\partial\xi^2}\right)-(1+\chi_2^2)\frac{\partial^2\bar{u}_2^L}{\partial\xi^2}\\&+\overline{K}_L\left((\bar{u}_2^L-\bar{u}_1^L)-\mu^2\left(\frac{\partial^2\bar{u}_2^L}{\partial\xi^2}-\frac{\partial^2\bar{u}_1^L}{\partial\xi^2}\right)\right)=0;\ 0<\xi<\bar{c}_2,\end{aligned} \tag{9c}$$

$$\begin{aligned}&(1+\chi_1^2)\left(\frac{\partial^2\bar{u}_2^R}{\partial\tau^2}-\mu^2\frac{\partial^4\bar{u}_2^R}{\partial\tau^2\partial\xi^2}\right)-(1+\chi_2^2)\frac{\partial^2\bar{u}_2^R}{\partial\xi^2}\\&+\overline{K}_L\left((\bar{u}_2^R-\bar{u}_1^L)-\mu^2\left(\frac{\partial^2\bar{u}_2^R}{\partial\xi^2}-\frac{\partial^2\bar{u}_1^L}{\partial\xi^2}\right)\right)(\mathrm{H}(\bar{c}_1-\xi)-\mathrm{H}(\bar{c}_2-\xi))+\overline{K}_L\\&\times\left((\bar{u}_2^R-\bar{u}_1^R)-\mu^2\left(\frac{\partial^2\bar{u}_2^R}{\partial\xi^2}-\frac{\partial^2\bar{u}_1^R}{\partial\xi^2}\right)\right)(1-\mathrm{H}(\bar{c}_1-\xi))=0;\ \bar{c}_2<\xi<1,\end{aligned} \tag{9d}$$

and for the case of $\bar{c}_1\leqslant\bar{c}_2$, the governing equations of the defected nanosystem are:

$$\begin{aligned}&(1+\chi_1^2)\left(\frac{\partial^2\bar{u}_1^L}{\partial\tau^2}-\mu^2\frac{\partial^4\bar{u}_1^L}{\partial\tau^2\partial\xi^2}\right)-(1+\chi_2^2)\frac{\partial^2\bar{u}_1^L}{\partial\xi^2}\\&+\overline{K}_L\left((\bar{u}_1^L-\bar{u}_2^L)-\mu^2\left(\frac{\partial^2\bar{u}_1^L}{\partial\xi^2}-\frac{\partial^2\bar{u}_2^L}{\partial\xi^2}\right)\right)=0;\ 0<\xi<\bar{c}_1,\end{aligned} \tag{10a}$$

$$\begin{aligned}&(1+\chi_1^2)\left(\frac{\partial^2\bar{u}_1^R}{\partial\tau^2}-\mu^2\frac{\partial^4\bar{u}_1^R}{\partial\tau^2\partial\xi^2}\right)-(1+\chi_2^2)\frac{\partial^2\bar{u}_1^R}{\partial\xi^2}\\&+\overline{K}_L\left((\bar{u}_1^R-\bar{u}_2^L)-\mu^2\left(\frac{\partial^2\bar{u}_1^R}{\partial\xi^2}-\frac{\partial^2\bar{u}_2^L}{\partial\xi^2}\right)\right)(\mathrm{H}(\bar{c}_2-\xi)-\mathrm{H}(\bar{c}_1-\xi))+\overline{K}_L\\&\times\left((\bar{u}_1^R-\bar{u}_2^R)-\mu^2\left(\frac{\partial^2\bar{u}_1^R}{\partial\xi^2}-\frac{\partial^2\bar{u}_2^R}{\partial\xi^2}\right)\right)(1-\mathrm{H}(\bar{c}_2-\xi))=0;\ \bar{c}_1<\xi<1,\end{aligned} \tag{10b}$$

$$\begin{aligned}&(1+\chi_1^2)\left(\frac{\partial^2\bar{u}_2^L}{\partial\tau^2}-\mu^2\frac{\partial^4\bar{u}_2^L}{\partial\tau^2\partial\xi^2}\right)-(1+\chi_2^2)\frac{\partial^2\bar{u}_2^L}{\partial\xi^2}\\&+\overline{K}_L\left((\bar{u}_2^L-\bar{u}_1^L)-\mu^2\left(\frac{\partial^2\bar{u}_2^L}{\partial\xi^2}-\frac{\partial^2\bar{u}_1^L}{\partial\xi^2}\right)\right)\mathrm{H}(\bar{c}_1-\xi)+\overline{K}_L\\&\times\left((\bar{u}_2^L-\bar{u}_1^R)-\mu^2\left(\frac{\partial^2\bar{u}_2^L}{\partial\xi^2}-\frac{\partial^2\bar{u}_1^R}{\partial\xi^2}\right)\right)(\mathrm{H}(\bar{c}_2-\xi)-\mathrm{H}(\bar{c}_1-\xi))=0;\ 0<\xi<\bar{c}_2,\end{aligned} \tag{10c}$$

$$\begin{aligned}&(1+\chi_1^2)\left(\frac{\partial^2\bar{u}_2^R}{\partial\tau^2}-\mu^2\frac{\partial^4\bar{u}_2^R}{\partial\tau^2\partial\xi^2}\right)-(1+\chi_2^2)\frac{\partial^2\bar{u}_2^R}{\partial\xi^2}\\&+\overline{K}_L\left((\bar{u}_2^R-\bar{u}_1^R)-\mu^2\left(\frac{\partial^2\bar{u}_2^R}{\partial\xi^2}-\frac{\partial^2\bar{u}_1^R}{\partial\xi^2}\right)\right)=0;\ \bar{c}_2<\xi<1,\end{aligned} \tag{10d}$$

with the following dimensionless nonclassical conditions at the local defects (i.e., $\xi=\bar{c}_1$and$\bar{c}_2$):

$$\begin{aligned}\bar{k}_1\left[\bar{u}_1^R(\bar{c}_1,\tau)-\bar{u}_1^L(\bar{c}_1,\tau)\right]=&\left[(1+\chi_2^2)+\mu^2(1+\chi_1^2)\frac{\partial^2}{\partial\tau^2}\right]\frac{\partial\bar{u}_1^L}{\partial\xi}(\bar{c}_1,\tau)\\&+\mu^2\overline{K}_L\left(\frac{\partial\bar{u}_1^L}{\partial\xi}(\bar{c}_1,\tau)-\frac{\partial\bar{u}_2^R}{\partial\xi}(\bar{c}_1,\tau)\right),\end{aligned} \tag{11a}$$

$$\begin{aligned}&\left[(1+\chi_2^2)+\mu^2(1+\chi_1^2)\frac{\partial^2}{\partial\tau^2}\right]\frac{\partial\bar{u}_1^L}{\partial\xi}(\bar{c}_1,\tau)+\mu^2\overline{K}_L\left(\frac{\partial\bar{u}_1^L}{\partial\xi}(\bar{c}_1,\tau)-\frac{\partial\bar{u}_2^R}{\partial\xi}(\bar{c}_1,\tau)\right)\\&=\left[(1+\chi_2^2)+\mu^2(1+\chi_1^2)\frac{\partial^2}{\partial\tau^2}\right]\frac{\partial\bar{u}_1^R}{\partial\xi}(\bar{c}_1,\tau)+\mu^2\overline{K}_L\left(\frac{\partial\bar{u}_1^R}{\partial\xi}(\bar{c}_1,\tau)-\frac{\partial\bar{u}_2^R}{\partial\xi}(\bar{c}_1,\tau)\right),\end{aligned} \tag{11b}$$

$$\begin{aligned}\bar{k}_2\left[\bar{u}_2^R(\bar{c}_2,\tau)-\bar{u}_2^L(\bar{c}_2,\tau)\right]=&\left[(1+\chi_2^2)+\mu^2(1+\chi_1^2)\frac{\partial^2}{\partial\tau^2}\right]\frac{\partial\bar{u}_2^L}{\partial\xi}(\bar{c}_2,\tau)\\&+\mu^2\overline{K}_L\left(\frac{\partial\bar{u}_2^L}{\partial\xi}(\bar{c}_2,\tau)-\frac{\partial\bar{u}_1^L}{\partial\xi}(\bar{c}_2,\tau)\right),\end{aligned} \tag{11c}$$

$$\begin{aligned}&\left[(1+\chi_2^2)+\mu^2(1+\chi_1^2)\frac{\partial^2}{\partial\tau^2}\right]\frac{\partial\bar{u}_2^L}{\partial\xi}(\bar{c}_2,\tau)+\mu^2\overline{K}_L\left(\frac{\partial\bar{u}_2^L}{\partial\xi}(\bar{c}_2,\tau)-\frac{\partial\bar{u}_1^L}{\partial\xi}(\bar{c}_2,\tau)\right)\\&=\left[(1+\chi_2^2)+\mu^2(1+\chi_1^2)\frac{\partial^2}{\partial\tau^2}\right]\frac{\partial\bar{u}_2^R}{\partial\xi}(\bar{c}_2,\tau)+\mu^2\overline{K}_L\left(\frac{\partial\bar{u}_2^R}{\partial\xi}(\bar{c}_2,\tau)-\frac{\partial\bar{u}_1^L}{\partial\xi}(\bar{c}_2,\tau)\right).\end{aligned} \tag{11d}$$

Eqs. (9a)–(9d) represent four coupled partial differential equations of second-order that should be solved with the boundary conditions given in Eqs. (11a)–(11d). It is worth mentioning that the proposed nonlocal-differential-based model can be readily reduced to the classical one as $e_0a\to0$.

In the following part, we employ the Galerkin approach based on admissible modes to study free longitudinal vibration of the defected nanosystem using the developed equations in this part.

2.2. Frequency analysis using Galerkin method on the basis of admissible modes

Let us to discretize the dimensionless-longitudinal displacements of the constitutive segments of the nanosystem in terms of admissible modes:

$$\begin{aligned}&\bar{u}_1^L(\xi,\tau)=\sum_{i=1}^{NM}\bar{a}_i(\tau)\varphi_i^{(1L)}(\xi),\ \bar{u}_1^R(\xi,\tau)=\sum_{i=1}^{NM}\bar{b}_i(\tau)\varphi_i^{(1R)}(\xi),\\&\bar{u}_2^L(\xi,\tau)=\sum_{i=1}^{NM}\bar{c}_i(\tau)\varphi_i^{(2L)}(\xi),\ \bar{u}_2^R(\xi,\tau)=\sum_{i=1}^{NM}\bar{d}_i(\tau)\varphi_i^{(2R)}(\xi),\end{aligned} \tag{12}$$

where $\varphi_i^{(jL)}(\xi)$ and $\varphi_i^{(jR)}(\xi)$ represent the ith admissible modes of the left-hand-side and right-hand-side of the local defect of the jth nanorod, respectively, $\bar{a}_i(\tau), \bar{b}_i(\tau), \bar{c}_i(\tau)$, and $\bar{d}_i(\tau)$ are the time-dependent parameters, and NM is the number of considered modes. The details of evaluation of the above-mentioned admissible modes for locally defected nanosystems with fixed–fixed and fixed-free end conditions have been explained in Appendix A.

The variation of the displacement fields in Eq. (12) are readily given by:

$$\begin{aligned}
&\delta\bar{u}_1^L(\xi,\tau)=\sum_{i=1}^{NM}\delta\bar{a}_i(\tau)\,\varphi_i^{(1L)}(\xi),\ \ \delta\bar{u}_1^R(\xi,\tau)=\sum_{i=1}^{NM}\delta\bar{b}_i(\tau)\,\varphi_i^{(1R)}(\xi),\\
&\delta\bar{u}_2^L(\xi,\tau)=\sum_{i=1}^{NM}\delta\bar{c}_i(\tau)\,\varphi_i^{(2L)}(\xi),\ \ \delta\bar{u}_2^R(\xi,\tau)=\sum_{i=1}^{NM}\delta\bar{d}_i(\tau)\,\varphi_i^{(2R)}(\xi),
\end{aligned}\tag{13}$$

where δ denotes the variational sign. Now Galerkin approach is employed to reduce the partial differential equations of motion to the ordinary differential equations. Without loss of generality, we proceed with the case of $\bar{c}_1 \geqslant \bar{c}_2$:

$$\int_0^{\bar{c}_1}\delta\bar{u}_1^L(\text{Eq.}(9a))\mathrm{d}\xi=0,\tag{14a}$$

$$\int_{\bar{c}_1}^1\delta\bar{u}_1^R(\text{Eq.}(9b))\mathrm{d}\xi=0,\tag{14b}$$

$$\int_0^{\bar{c}_2}\delta\bar{u}_2^L(\text{Eq.}(9c))\mathrm{d}\xi=0,\tag{14c}$$

$$\int_{\bar{c}_2}^1\delta\bar{u}_2^R(\text{Eq.}(9d))\mathrm{d}\xi=0.\tag{14d}$$

By substitution of Eqs. (9a)–(9d), (12) and (13) into Eqs. (14a)–(14d),

$$\begin{aligned}
&\left((1+\chi_1^2)\left(\int_0^{\bar{c}_1}\varphi_i^{(1L)}\varphi_j^{(1L)}\mathrm{d}\xi-\mu^2\int_0^{\bar{c}_1}\varphi_i^{(1L)}\varphi_{j,\xi\xi}^{(1L)}\mathrm{d}\xi\right)\right)\bar{a}_{j,\tau\tau}\\
&+\left(-(1+\chi_2^2)\int_0^{\bar{c}_1}\varphi_i^{(1L)}\varphi_{j,\xi\xi}^{(1L)}\mathrm{d}\xi+\overline{K}_L\left(\frac{\int_0^{\bar{c}_1}\mathrm{H}(\bar{c}_1-\xi)\varphi_i^{(1L)}\varphi_j^{(1L)}\mathrm{d}\xi-}{\mu^2\int_0^{\bar{c}_1}\mathrm{H}(\bar{c}_1-\xi)\varphi_i^{(1L)}\varphi_{j,\xi\xi}^{(1L)}\mathrm{d}\xi}\right)\right)\bar{a}_j\\
&+\left(-\overline{K}_L\left(\int_0^{\bar{c}_1}\mathrm{H}(\bar{c}_2-\xi)\varphi_i^{(1L)}\varphi_j^{(2L)}\mathrm{d}\xi-\mu^2\int_0^{\bar{c}_1}\mathrm{H}(\bar{c}_2-\xi)\varphi_i^{(1L)}\varphi_{j,\xi\xi}^{(2L)}\mathrm{d}\xi\right)\right)\bar{c}_j\\
&+\left(-\overline{K}_L\left(\frac{\int_0^{\bar{c}_1}(\mathrm{H}(\bar{c}_1-\xi)-\mathrm{H}(\bar{c}_2-\xi))\varphi_i^{(1L)}\varphi_j^{(2R)}\mathrm{d}\xi-}{\mu^2\int_0^{\bar{c}_1}(\mathrm{H}(\bar{c}_1-\xi)-\mathrm{H}(\bar{c}_2-\xi))\varphi_i^{(1L)}\varphi_{j,\xi\xi}^{(2R)}\mathrm{d}\xi}\right)\right)\bar{d}_j=0,
\end{aligned}\tag{15a}$$

$$\begin{aligned}
&\left((1+\chi_1^2)\left(\int_{\bar{c}_1}^1\varphi_i^{(1R)}\varphi_j^{(1R)}\mathrm{d}\xi-\mu^2\int_{\bar{c}_1}^1\varphi_i^{(1R)}\varphi_{j,\xi\xi}^{(1R)}\mathrm{d}\xi\right)\right)\bar{b}_{j,\tau\tau}\\
&+\left(-(1+\chi_2^2)\int_{\bar{c}_1}^1\varphi_i^{(1R)}\varphi_{j,\xi\xi}^{(1R)}\mathrm{d}\xi+\overline{K}_L\left(\frac{\int_{\bar{c}_1}^1\varphi_i^{(1R)}\varphi_j^{(1R)}\mathrm{d}\xi-}{\mu^2\int_{\bar{c}_1}^1\varphi_i^{(1R)}\varphi_{j,\xi\xi}^{(1R)}\mathrm{d}\xi}\right)\right)\bar{b}_j\\
&+\left(-\overline{K}_L\left(\int_{\bar{c}_1}^1\varphi_i^{(1R)}\varphi_j^{(2R)}\mathrm{d}\xi-\mu^2\int_{\bar{c}_1}^1\varphi_i^{(1R)}\varphi_{j,\xi\xi}^{(2R)}\mathrm{d}\xi\right)\right)\bar{d}_j=0,
\end{aligned}\tag{15b}$$

$$\begin{aligned}
&\left((1+\chi_1^2)\left(\int_0^{\bar{c}_2}\varphi_i^{(2L)}\varphi_j^{(2L)}\mathrm{d}\xi-\mu^2\int_0^{\bar{c}_2}\varphi_i^{(2L)}\varphi_{j,\xi\xi}^{(2L)}\mathrm{d}\xi\right)\right)\bar{c}_{j,\tau\tau}\\
&+\left(-\overline{K}_L\left(\int_0^{\bar{c}_2}\varphi_i^{(2L)}\varphi_j^{(1L)}\mathrm{d}\xi-\mu^2\int_0^{\bar{c}_2}\varphi_i^{(2L)}\varphi_{j,\xi\xi}^{(L)}\mathrm{d}\xi\right)\right)\bar{a}_j\\
&+\left(-(1+\chi_2^2)\int_0^{\bar{c}_2}\varphi_i^{(2L)}\varphi_{j,\xi\xi}^{(2L)}\mathrm{d}\xi+\overline{K}_L\left(\frac{\int_0^{\bar{c}_2}\varphi_i^{(2L)}\varphi_j^{(2L)}\mathrm{d}\xi-}{\mu^2\int_0^{\bar{c}_2}\varphi_i^{(2L)}\varphi_{j,\xi\xi}^{(2L)}\mathrm{d}\xi}\right)\right)\bar{c}_j=0,
\end{aligned}\tag{15c}$$

$$\begin{aligned}
&\left((1+\chi_1^2)\left(\int_{\bar{c}_2}^1\varphi_i^{(2R)}\varphi_j^{(2R)}\mathrm{d}\xi-\mu^2\int_{\bar{c}_2}^1\varphi_i^{(2R)}\varphi_{j,\xi\xi}^{(2R)}\mathrm{d}\xi\right)\right)\bar{d}_{j,\tau\tau}\\
&+\left(-\overline{K}_L\left(\frac{\int_{\bar{c}_2}^1(\mathrm{H}(\bar{c}_1-\xi)-\mathrm{H}(\bar{c}_2-\xi))\varphi_i^{(2R)}\varphi_{j,\xi\xi}^{(1L)}\mathrm{d}\xi-}{\mu^2\int_{\bar{c}_2}^1(\mathrm{H}(\bar{c}_1-\xi)-\mathrm{H}(\bar{c}_2-\xi))\varphi_i^{(2R)}\varphi_{j,\xi\xi}^{(1L)}\mathrm{d}\xi}\right)\right)\bar{a}_j\\
&+\left(-\overline{K}_L\left(\frac{\int_{\bar{c}_2}^1(1-\mathrm{H}(\bar{c}_2-\xi))\varphi_i^{(2R)}\varphi_j^{(1R)}\mathrm{d}\xi-}{\mu^2\int_{\bar{c}_2}^1(1-\mathrm{H}(\bar{c}_2-\xi))\varphi_i^{(2R)}\varphi_{j,\xi\xi}^{(1R)}\mathrm{d}\xi}\right)\right)\bar{b}_j\\
&+\left(-(1+\chi_2^2)\int_0^{\bar{c}_1}\varphi_i^{(2R)}\varphi_{j,\xi\xi}^{(2R)}\mathrm{d}\xi+\overline{K}_L\left(\frac{\int_{\bar{c}_2}^1(1-\mathrm{H}(\bar{c}_2-\xi))\varphi_i^{(2R)}\varphi_j^{(2R)}\mathrm{d}\xi-}{\mu^2\int_{\bar{c}_2}^1(1-\mathrm{H}(\bar{c}_2-\xi))\varphi_i^{(2R)}\varphi_{j,\xi\xi}^{(2R)}\mathrm{d}\xi}\right)\right)\bar{d}_j=0,
\end{aligned}\tag{15d}$$

or in the matrix form:

$$\overline{\mathbf{M}}\frac{\mathrm{d}^2\bar{\mathbf{x}}}{\mathrm{d}\tau^2}+\overline{\mathbf{K}}\bar{\mathbf{x}}=\mathbf{0},\tag{16}$$

where

$$\overline{\mathbf{M}}=\begin{pmatrix}\bar{M}_{ij}^{(11)} & \bar{M}_{ij}^{(12)} & \bar{M}_{ij}^{(13)} & \bar{M}_{ij}^{(14)}\\ \bar{M}_{ij}^{(21)} & \bar{M}_{ij}^{(22)} & \bar{M}_{ij}^{(23)} & \bar{M}_{ij}^{(24)}\\ \bar{M}_{ij}^{(31)} & \bar{M}_{ij}^{(32)} & \bar{M}_{ij}^{(33)} & \bar{M}_{ij}^{(34)}\\ \bar{M}_{ij}^{(41)} & \bar{M}_{ij}^{(42)} & \bar{M}_{ij}^{(43)} & \bar{M}_{ij}^{(44)}\end{pmatrix},\ \overline{\mathbf{K}}=\begin{pmatrix}\bar{K}_{ij}^{(11)} & \bar{K}_{ij}^{(12)} & \bar{K}_{ij}^{(13)} & \bar{K}_{ij}^{(14)}\\ \bar{K}_{ij}^{(21)} & \bar{K}_{ij}^{(22)} & \bar{K}_{ij}^{(23)} & \bar{K}_{ij}^{(24)}\\ \bar{K}_{ij}^{(31)} & \bar{K}_{ij}^{(32)} & \bar{K}_{ij}^{(33)} & \bar{K}_{ij}^{(34)}\\ \bar{K}_{ij}^{(41)} & \bar{K}_{ij}^{(42)} & \bar{K}_{ij}^{(43)} & \bar{K}_{ij}^{(44)}\end{pmatrix},\ \bar{\mathbf{x}}=\begin{pmatrix}\bar{\mathbf{a}}\\ \bar{\mathbf{b}}\\ \bar{\mathbf{c}}\\ \bar{\mathbf{d}}\end{pmatrix},\tag{17}$$

where the nonvanishing dimensionless mass and stiffness submatrices for the case of $\bar{c}_1 \geqslant \bar{c}_2$ as well as the dimensionless vectors of the unknown-parameters are as:

$$\overline{M}_{ij}^{(11)}=(1+\chi_1^2)\left(1+\left(\lambda_j^{(1)}\mu\right)^2\right)\int_0^{\bar{c}_1}\varphi_i^{(1L)}\varphi_j^{(1L)}\mathrm{d}\xi,\tag{18a}$$

$$\overline{M}_{ij}^{(22)}=(1+\chi_1^2)\left(1+\left(\lambda_j^{(1)}\mu\right)^2\right)\int_{\bar{c}_1}^1\varphi_i^{(1R)}\varphi_j^{(1R)}\mathrm{d}\xi,\tag{18b}$$

$$\overline{M}_{ij}^{(33)}=(1+\chi_1^2)\left(1+\left(\lambda_j^{(2)}\mu\right)^2\right)\int_0^{\bar{c}_2}\varphi_i^{(2L)}\varphi_j^{(2L)}\mathrm{d}\xi,\tag{18c}$$

$$\overline{M}_{ij}^{(44)}=(1+\chi_1^2)\left(1+\left(\lambda_j^{(2)}\mu\right)^2\right)\int_{\bar{c}_2}^1\varphi_i^{(2R)}\varphi_j^{(2R)}\mathrm{d}\xi,\tag{18d}$$

$$\begin{aligned}
\overline{K}_{ij}^{(11)}=\ &(1+\chi_2^2)\left(\lambda_j^{(1)}\right)^2\int_0^{\bar{c}_1}\varphi_i^{(1L)}\varphi_j^{(1L)}\mathrm{d}\xi\\
&+\bar{K}_L\left(1+\left(\mu\lambda_j^{(1)}\right)^2\right)\int_0^{\bar{c}_1}\mathrm{H}(\bar{c}_1-\xi)\varphi_i^{(1L)}\varphi_j^{(1L)}\mathrm{d}\xi,
\end{aligned}\tag{18e}$$

$$\overline{K}_{ij}^{(13)}=-\bar{K}_L\left(1+\left(\mu\lambda_j^{(2)}\right)^2\right)\int_0^{\bar{c}_1}\mathrm{H}(\bar{c}_2-\xi)\varphi_i^{(1L)}\varphi_j^{(2L)}\mathrm{d}\xi,\tag{18f}$$

$$\overline{K}_{ij}^{(14)}=-\bar{K}_L\left(1+\left(\mu\lambda_j^{(2)}\right)^2\right)\int_0^{\bar{c}_1}(\mathrm{H}(\bar{c}_1-\xi)-\mathrm{H}(\bar{c}_2-\xi))\varphi_i^{(1L)}\varphi_j^{(2R)}\mathrm{d}\xi,\tag{18g}$$

$$\overline{K}_{ij}^{(22)}=\left(((1+\chi_2^2)+\overline{K}_L\mu^2)\left(\lambda_j^{(1)}\right)^2+\overline{K}_L\right)\int_{\bar{c}_1}^1\varphi_i^{(1R)}\varphi_j^{(1R)}\mathrm{d}\xi,\tag{18h}$$

$$\overline{K}_{ij}^{(24)}=-\bar{K}_L\left(1+\left(\mu\lambda_j^{(2)}\right)^2\right)\int_{\bar{c}_1}^1\varphi_i^{(1R)}\varphi_j^{(2R)}\mathrm{d}\xi,\tag{18i}$$

$$\overline{K}_{ij}^{(31)}=-\bar{K}_L\left(1+\left(\mu\lambda_j^{(1)}\right)^2\right)\int_0^{\bar{c}_2}\varphi_i^{(2L)}\varphi_j^{(1L)}\mathrm{d}\xi,\tag{18j}$$

$$\overline{K}_{ij}^{(33)}=\left(((1+\chi_2^2)+\overline{K}_L\mu^2)\left(\lambda_j^{(2)}\right)^2+\overline{K}_L\right)\int_0^{\bar{c}_2}\varphi_i^{(2L)}\varphi_j^{(2L)}\mathrm{d}\xi,\tag{18k}$$

$$\overline{K}_{ij}^{(41)}=-\bar{K}_L\left(1+\left(\mu\lambda_j^{(1)}\right)^2\right)\int_{\bar{c}_2}^1(\mathrm{H}(\bar{c}_1-\xi)-\mathrm{H}(\bar{c}_2-\xi))\varphi_i^{(2R)}\varphi_j^{(1L)}\mathrm{d}\xi,\tag{18l}$$

$$\overline{K}_{ij}^{(42)}=-\bar{K}_L\left(1+\left(\mu\lambda_j^{(1)}\right)^2\right)\int_{\bar{c}_2}^1(1-\mathrm{H}(\bar{c}_1-\xi))\varphi_i^{(2R)}\varphi_j^{(1R)}\mathrm{d}\xi,\tag{18m}$$

$$\begin{aligned}
\overline{K}_{ij}^{(44)}=\ &(1+\chi_2^2)\left(\lambda_j^{(2)}\right)^2\int_{\bar{c}_2}^1\varphi_i^{(2R)}\varphi_j^{(2R)}\mathrm{d}\xi\\
&+\bar{K}_L\left(1+\left(\mu\lambda_j^{(2)}\right)^2\right)\int_{\bar{c}_2}^1(1-\mathrm{H}(\bar{c}_2-\xi))\varphi_i^{(2R)}\varphi_j^{(2R)}\mathrm{d}\xi,
\end{aligned}\tag{18n}$$

$$\bar{\mathbf{a}}(\tau)=<\bar{a}_1(\tau),\bar{a}_2(\tau),\ldots,\bar{a}_{NM}(\tau)>^{\mathrm{T}},\tag{18o}$$

$$\bar{\mathbf{b}}(\tau)=<\bar{b}_1(\tau),\bar{b}_2(\tau),\ldots,\bar{b}_{NM}(\tau)>^{\mathrm{T}},\tag{18p}$$

$$\bar{\mathbf{c}}(\tau)=<\bar{c}_1(\tau),\bar{c}_2(\tau),\ldots,\bar{c}_{NM}(\tau)>^{\mathrm{T}},\tag{18q}$$

$$\bar{\mathbf{d}}(\tau) = <\bar{d}_1(\tau), \bar{d}_2(\tau), \ldots, \bar{d}_{NM}(\tau)>^{\mathrm{T}}, \tag{18r}$$

in which the vibration modes of the left-hand-side and the right-hand-side of the local defect of the jth locally defected nanorod with the fixed–fixed and fixed-free ends are as follows (see Appendix A):

1. fixed–fixed:

$$\begin{aligned}\varphi_i^{(jL)} &= \sin\left(\lambda_i^{(j)}\xi\right);\ j = 1, 2,\\ \varphi_i^{(jR)} &= \sin\left(\lambda_i^{(j)}\right)\cos\left(\lambda_i^{(j)}\xi\right) - \cos\left(\lambda_i^{(j)}\right)\sin\left(\lambda_i^{(j)}\xi\right),\end{aligned} \tag{19}$$

1. fixed-free:

$$\begin{aligned}\varphi_i^{(jL)} &= \sin\left(\lambda_i^{(j)}\xi\right),\\ \varphi_i^{(jR)} &= \cos\left(\lambda_i^{(j)}\right)\cos\left(\lambda_i^{(j)}\xi\right) + \sin\left(\lambda_i^{(j)}\right)\sin\left(\lambda_i^{(j)}\xi\right),\end{aligned} \tag{20}$$

and the values of $\lambda_i^{(j)}$ are given by Eq. (A.11).

In order to solve the set of $4NM$ ordinary differential equations in Eq. (16) for longitudinal frequency, the following harmonic form is considered for the time-dependent vector: $\bar{\mathbf{x}} = \bar{\mathbf{x}}_0 e^{i\varpi\tau}$. By substituting this version of $\bar{\mathbf{x}}$ into Eq. (16), we will arrive at: $\det(-\varpi^2\mathbf{M} + \mathbf{K}) = 0$, and therefore, the linear longitudinal frequencies are readily determined.

3. Development of a nonlocal-integral-based mathematical model

3.1. Nonlocal-integral-surface energy-based governing equations

Using the nonlocal-integro-based constitutive equations for one-dimensional nanorods, the nonlocal stress within the bulk and the surface of the ith nanorod (i.e., $\sigma_{b,i}^{nl}$ and $\sigma_{s,i}^{nl}$) could be related to their local values (i.e., $\sigma_{b,i}^{l}$ and $\sigma_{s,i}^{l}$) by:

$$\sigma_{b,i}^{nl}(\mathbf{x}, t) = \int_{\Omega}\Gamma_b(|\mathbf{x}^* - \mathbf{x}|; e_0 a)\,\sigma_{b,i}^{l}(\mathbf{x}^*, t)\,\mathrm{d}\Omega^*, \tag{21a}$$

$$\sigma_{s,i}^{nl}(\mathbf{x}, t) = \int_{\mathscr{S}}\Gamma_s(|\mathbf{x}^* - \mathbf{x}|; e_0 a)\,\sigma_{s,i}^{l}(\mathbf{x}^*, t)\,\mathrm{d}\mathscr{S}^*, \tag{21b}$$

where $|\mathbf{x}^* - \mathbf{x}|$ represents the euclidean distance between two points of coordinates $\mathbf{x}$ and $\mathbf{x}^*$ from the equivalent continuum associated with the nanorod, $\Gamma_b = \Gamma_b(|\mathbf{x}^* - \mathbf{x}|; e_0 a)$ and $\Gamma_s = \Gamma_s(|\mathbf{x}^* - \mathbf{x}|; e_0 a)$ denote the kernel functions associated with the bulk and the surface. By assuming uniform distribution of the local axial stress across the cross-section of the continuum-based nanorods, both local and nonlocal stress fields of the constitutive nanorods of the nanosystem at hand would be only x-dependent.

Now by defining the kernel functions as: $\Gamma_b = \Gamma_{b0}\,g(|x|; e_0 a)$ and $\Gamma_s = \Gamma_{s0}\,g(|x|; e_0 a)$ where g is the attenuating function, Eqs. (21a) and (21b) can be rewritten as follows:

$$\sigma_{b,i}^{nl}(x, t) = \int_0^{l_b}\Gamma_{b0}\,g(|x^* - x|; e_0 a)\,\sigma_{b,i}^{l}(x^*, t)\,\mathrm{d}x^*, \tag{22a}$$

$$\sigma_{s,i}^{nl}(x, t) = \int_0^{l_b}\Gamma_{s0}\,g(|x^* - x|; e_0 a)\,\sigma_{s,i}^{l}(x^*, t)\,\mathrm{d}x^*, \tag{22b}$$

where the most common attenuating functions are as [12]:

$$g(x; e_0 a) = \exp\left(-\tfrac{|x|}{e_0 a}\right), \exp\left(-\left(k\tfrac{|x|}{e_0 a}\right)^2\right), \left(1 - \tfrac{|x|}{e_0 a}\right)\mathrm{H}\left(1 - \tfrac{|x|}{e_0 a}\right), \tag{23}$$

where $k = 1.65$, $\Gamma_{b0} = \Gamma_0/A_b$ and $\Gamma_{s0} = \Gamma_0/A_0$ such that $\Gamma_0 = \left[\int_{-\infty}^{\infty} g(|x^*|; e_0 a)\,\mathrm{d}x^*\right]^{-1}$.

The nonlocal longitudinal force within the ith nanorod is computed by: $N_i^{nl}(x, t) = \int_{A_b}\sigma_{b,i}^{nl}(x, t)\,\mathrm{d}A_b + \int_{A_s}\sigma_{s,i}^{nl}(x, t)\,\mathrm{d}A_s$. By substituting Eqs. (22a) and (22b) into this relation, it is obtained:

$$N_i^{nl}(x, t) = (E_b A_b + E_0 A_0)\int_{x^*=0}^{l_b}\Gamma_0\,g(|x^* - x|, e_0 a)\,\frac{\partial u_i}{\partial x}(x^*, t)\,\mathrm{d}x^*. \tag{24}$$

By introducing Eq. (24) to Eqs. (2) and (3), the elastic strain energy of the defected nanosystem on the basis of the nonlocal-integral-elasticity theory of Eringen for the case of $c_1 \geqslant c_2$ takes the following form:

$$\begin{aligned}U(t) = {} & \tfrac{1}{2}(E_b A_b + E_0 A_0)\sum_{i=1}^{2}\int_0^{c_i}\int_0^{c_i}\Gamma_0\,g(|x^* - x|, e_0 a)\,\frac{\partial u_i^L}{\partial x}(x^*, t)\,\frac{\partial u_i^L}{\partial x}(x, t)\,\mathrm{d}x^*\mathrm{d}x\\ & + \tfrac{1}{2}(E_b A_b + E_0 A_0)\sum_{i=1}^{2}\int_{c_i}^{l_b}\int_{c_i}^{l_b}\Gamma_0\,g(|x^* - x|, e_0 a)\,\frac{\partial u_i^R}{\partial x}(x^*, t)\,\frac{\partial u_i^R}{\partial x}(x, t)\,\mathrm{d}x^*\mathrm{d}x\\ & + \tfrac{1}{2}\int_0^{c_2}K_L\left(u_1^L - u_2^L\right)^2\mathrm{d}x + \tfrac{1}{2}\int_{c_2}^{c_1}K_L\left(u_1^L - u_2^R\right)^2\mathrm{d}x\\ & + \tfrac{1}{2}\int_{c_1}^{l_b}K_L\left(u_2^R - u_2^R\right)^2\mathrm{d}x + \tfrac{1}{2}\sum_{i=1}^{2}k_i\left(u_i^L(c_i, t) - u_i^R(c_i, t)\right)^2,\end{aligned} \tag{25}$$

and in the case of $c_1 \leqslant c_2$, it is expressed by:

$$\begin{aligned}U(t) = {} & \tfrac{1}{2}(E_b A_b + E_0 A_0)\sum_{i=1}^{2}\int_0^{c_i}\int_0^{c_i}\Gamma_0\,g(|x^* - x|, e_0 a)\,\frac{\partial u_i^L}{\partial x}(x^*, t)\,\frac{\partial u_i^L}{\partial x}(x, t)\,\mathrm{d}x^*\mathrm{d}x\\ & + \tfrac{1}{2}(E_b A_b + E_0 A_0)\sum_{i=1}^{2}\int_{c_i}^{l_b}\int_{c_i}^{l_b}\Gamma_0\,g(|x^* - x|, e_0 a)\,\frac{\partial u_i^R}{\partial x}(x^*, t)\,\frac{\partial u_i^R}{\partial x}(x, t)\,\mathrm{d}x^*\mathrm{d}x\\ & + \tfrac{1}{2}\int_0^{c_1}K_L\left(u_1^L - u_2^L\right)^2\mathrm{d}x + \tfrac{1}{2}\int_{c_1}^{c_2}K_L\left(u_1^R - u_2^L\right)^2\mathrm{d}x\\ & + \tfrac{1}{2}\int_{c_2}^{l_b}K_L\left(u_2^R - u_2^R\right)^2\mathrm{d}x + \tfrac{1}{2}\sum_{i=1}^{2}k_i\left(u_i^L(c_i, t) - u_i^R(c_i, t)\right)^2.\end{aligned} \tag{26}$$

Now by using the Hamilton's principle, in view of the given kinetic energy in Eq. (1), the nonlocal-integral-equations of motion of the constitutive segments of the defected nanosystem in the case of $c_1 \geqslant c_2$ take the following form:

$$\begin{aligned}&(\rho_b A_b + \rho_0 A_0)\frac{\partial^2 u_1^L}{\partial t^2} - (E_b A_b + E_0 A_0)\frac{\partial}{\partial x}\left[\int_0^{c_1}\Gamma_0\,g(|x^* - x|, e_0 a)\,\frac{\partial u_1^L}{\partial x}(x^*, t)\,\mathrm{d}x^*\right]\\ &+K_L\left(u_1^L - u_2^L\right)\mathrm{H}(c_2 - x) + K_L\left(u_1^L - u_2^R\right) = 0;\ 0 < x < c_1,\end{aligned} \tag{27a}$$

$$\begin{aligned}&(\rho_0 A_0 + \rho_0 A_0)\frac{\partial^2 u_1^R}{\partial t^2} - (E_b A_b + E_0 A_0)\frac{\partial}{\partial x}\left[\int_{c_1}^{l_b}\Gamma_0\,g(|x^* - x|, e_0 a)\,\frac{\partial u_1^R}{\partial x}(x^*, t)\,\mathrm{d}x^*\right]\\ &+K_L\left(u_1^R - u_2^R\right) = 0;\ c_1 < x < l_b,\end{aligned} \tag{27b}$$

$$\begin{aligned}&(\rho_b A_b + \rho_0 A_0)\frac{\partial^2 u_2^L}{\partial t^2} - (E_b A_b + E_0 A_0)\frac{\partial}{\partial x}\left[\int_0^{c_2}\Gamma_0\,g(|x^* - x|, e_0 a)\,\frac{\partial u_2^L}{\partial x}(x^*, t)\,\mathrm{d}x^*\right]\\ &+K_L\left(u_2^L - u_1^L\right) = 0;\ 0 < x < c_2,\end{aligned} \tag{27c}$$

$$\begin{aligned}&(\rho_b A_b + \rho_0 A_0)\frac{\partial^2 u_2^R}{\partial t^2} - (E_b A_b + E_0 A_0)\frac{\partial}{\partial x}\left[\int_{c_2}^{l_b}\Gamma_0\,g(|x^* - x|, e_0 a)\,\frac{\partial u_2^R}{\partial x}(x^*, t)\,\mathrm{d}x^*\right]\\ &+K_L\left(u_2^R - u_1^L\right)(\mathrm{H}(c_1 - x) - \mathrm{H}(c_2 - x))\\ &+K_L\left(u_2^R - u_1^R\right)(1 - \mathrm{H}(c_1 - x)) = 0;\ c_2 < x < l_b,\end{aligned} \tag{27d}$$

and in the case of $c_1 < c_2$, they are obtained as:

$$\begin{aligned}&(\rho_b A_b + \rho_0 A_0)\frac{\partial^2 u_1^L}{\partial t^2} - (E_b A_b + E_0 A_0)\frac{\partial}{\partial x}\left[\int_0^{c_1}\Gamma_0\,g(|x^* - x|, e_0 a)\,\frac{\partial u_1^L}{\partial x}(x^*, t)\,\mathrm{d}x^*\right]\\ &+K_L\left(u_1^L - u_2^L\right) = 0;\ 0 < x < c_1,\end{aligned} \tag{28a}$$

$$\begin{aligned}&(\rho_0 A_0 + \rho_0 A_0)\frac{\partial^2 u_1^R}{\partial t^2} - (E_b A_b + E_0 A_0)\frac{\partial}{\partial x}\left[\int_{c_1}^{l_b}\Gamma_0\,g(|x^* - x|, e_0 a)\,\frac{\partial u_1^R}{\partial x}(x^*, t)\,\mathrm{d}x^*\right]\\ &+K_L\left(u_1^R - u_2^L\right)(\mathrm{H}(c_2 - x) - \mathrm{H}(c_1 - x))\\ &+K_L\left(u_1^R - u_2^R\right)(1 - \mathrm{H}(c_2 - x)) = 0;\ c_1 < x < l_b,\end{aligned} \tag{28b}$$

$$\begin{aligned}&(\rho_b A_b + \rho_0 A_0)\frac{\partial^2 u_2^L}{\partial t^2} - (E_b A_b + E_0 A_0)\frac{\partial}{\partial x}\left[\int_0^{c_2}\Gamma_0\,g(|x^* - x|, e_0 a)\,\frac{\partial u_2^L}{\partial x}(x^*, t)\,\mathrm{d}x^*\right]\\ &+K_L\left(u_2^L - u_1^L\right)\mathrm{H}(c_1 - x) + K_L\left(u_2^L - u_1^R\right)(\mathrm{H}(c_2 - x) - \mathrm{H}(c_1 - x)) = 0;\ 0 < x < c_2,\end{aligned} \tag{28c}$$

$$\begin{aligned}&(\rho_b A_b + \rho_0 A_0)\frac{\partial^2 u_2^R}{\partial t^2} - (E_b A_b + E_0 A_0)\frac{\partial}{\partial x}\left[\int_{c_2}^{l_b}\Gamma_0\,g(|x^* - x|, e_0 a)\,\frac{\partial u_2^R}{\partial x}(x^*, t)\,\mathrm{d}x^*\right]\\ &+K_L\left(u_2^R - u_1^R\right) = 0;\ c_2 < x < l_b.\end{aligned} \tag{28d}$$

The boundary conditions at the segments' interfaces are as:

$$k_1\left(u_1^R(c_1,t)-u_1^L(c_1,t)\right) = (E_bA_b+E_0A_0)\int_0^{c_1}\Gamma_0 g(|x^*-c_1|,e_0a)\frac{\partial u_1^L}{\partial x}(x^*,t)\,\mathrm{d}x^*, \tag{29a}$$

$$(E_bA_b+E_0A_0)\int_0^{c_1}\Gamma_0 g(|x^*-c_1|,e_0a)\frac{\partial u_1^L}{\partial x}(x^*,t)\,\mathrm{d}x^* = (E_bA_b+E_0A_0)\int_{c_1}^{l_b}\Gamma_0 g(|x^*-c_1|,e_0a)\frac{\partial u_1^R}{\partial x}(x^*,t)\,\mathrm{d}x^*, \tag{29b}$$

$$k_2\left(u_2^R(c_2,t)-u_2^L(c_2,t)\right) = (E_bA_b+E_0A_0)\int_0^{c_2}\Gamma_0 g(|x^*-c_1|,e_0a)\frac{\partial u_2^L}{\partial x}(x^*,t)\,\mathrm{d}x^*, \tag{29c}$$

$$(E_bA_b+E_0A_0)\int_0^{c_2}\Gamma_0 g(|x^*-c_2|,e_0a)\frac{\partial u_2^L}{\partial x}(x^*,t)\,\mathrm{d}x^* = (E_bA_b+E_0A_0)\int_{c_2}^{l_b}\Gamma_0 g(|x^*-c_2|,e_0a)\frac{\partial u_2^R}{\partial x}(x^*,t)\,\mathrm{d}x^*. \tag{29d}$$

By implementing the given dimensionless quantities in Eq. (8), the dimensionless nonlocal-integral-equations of motion of the defected nanosystem in the case of $c_1 \geqslant c_2$ according to Eqs. (27a)–(27d) are provided by:

$$(1+\chi_1^2)\frac{\partial^2 u_1^L}{\partial\tau^2}-(1+\chi_2^2)\frac{\partial}{\partial\xi}\left[\int_0^{\bar{c}_1}\Gamma_0 g(|\xi^*-\xi|,\mu)\frac{\partial u_1^L}{\partial\xi}(\xi^*,\tau)\,\mathrm{d}\xi^*\right] +\bar{K}_L\left(\bar{u}_1^L-\bar{u}_2^L\right)\mathrm{H}(\bar{c}_2-\xi)+\bar{K}_L\left(\bar{u}_1^L-\bar{u}_2^R\right)=0;\ 0<\xi<\bar{c}_1, \tag{30a}$$

$$(1+\chi_1^2)\frac{\partial^2 u_1^R}{\partial\tau^2}-(1+\chi_2^2)\frac{\partial}{\partial\xi}\left[\int_{\bar{c}_1}^{1}\Gamma_0 g(|\xi^*-\xi|,\mu)\frac{\partial u_1^R}{\partial\xi}(\xi^*,\tau)\,\mathrm{d}\xi^*\right] +\bar{K}_L\left(\bar{u}_1^R-\bar{u}_2^R\right)=0;\ \bar{c}_1<\xi<1, \tag{30b}$$

$$(1+\chi_1^2)\frac{\partial^2 u_2^L}{\partial\tau^2}-(1+\chi_2^2)\frac{\partial}{\partial\xi}\left[\int_0^{\bar{c}_2}\Gamma_0 g(|\xi^*-\xi|,\mu)\frac{\partial u_2^L}{\partial\xi}(\xi^*,\tau)\,\mathrm{d}\xi^*\right] +\bar{K}_L\left(\bar{u}_2^L-\bar{u}_1^L\right)=0;\ 0<\xi<\bar{c}_2, \tag{30c}$$

$$(1+\chi_1^2)\frac{\partial^2 u_2^R}{\partial\tau^2}-(1+\chi_2^2)\frac{\partial}{\partial\xi}\left[\int_{\bar{c}_2}^{1}\Gamma_0 g(|\xi^*-\xi|,\mu)\frac{\partial u_2^R}{\partial\xi}(\xi^*,\tau)\,\mathrm{d}\xi^*\right] +\bar{K}_L\left(\bar{u}_2^R-\bar{u}_1^L\right)(\mathrm{H}(\bar{c}_1-\xi)-\mathrm{H}(\bar{c}_2-\xi))+\bar{K}_L\left(\bar{u}_2^R-\bar{u}_1^R\right)(1-\mathrm{H}(\bar{c}_1-\xi))=0;\ \bar{c}_2<\xi<1, \tag{30d}$$

and for the case of $c_1 < c_2$ based on Eqs. (28a)-(28d), the dimensionless governing equations are written by:

$$(1+\chi_1^2)\frac{\partial^2 u_1^L}{\partial\tau^2}-(1+\chi_2^2)\frac{\partial}{\partial\xi}\left[\int_0^{\bar{c}_1}\Gamma_0 g(|\xi^*-\xi|,\mu)\frac{\partial u_1^L}{\partial\xi}(\xi^*,\tau)\,\mathrm{d}\xi^*\right] +\bar{K}_L\left(\bar{u}_1^L-\bar{u}_2^L\right)=0;\ 0<\xi<\bar{c}_1, \tag{31a}$$

$$(1+\chi_1^2)\frac{\partial^2 u_1^R}{\partial\tau^2}-(1+\chi_2^2)\frac{\partial}{\partial\xi}\left[\int_{\bar{c}_1}^{1}\Gamma_0 g(|\xi^*-\xi|,\mu)\frac{\partial u_1^R}{\partial\xi}(\xi^*,\tau)\,\mathrm{d}\xi^*\right] +\bar{K}_L\left(\bar{u}_1^R-\bar{u}_2^L\right)(\mathrm{H}(\bar{c}_2-\xi)-\mathrm{H}(\bar{c}_1-\xi))+\bar{K}_L\left(\bar{u}_1^R-\bar{u}_2^R\right)(1-\mathrm{H}(\bar{c}_2-\xi))=0;\ \bar{c}_1<\xi<1, \tag{31b}$$

$$(1+\chi_1^2)\frac{\partial^2 u_2^L}{\partial\tau^2}-(1+\chi_2^2)\frac{\partial}{\partial\xi}\left[\int_0^{\bar{c}_2}\Gamma_0 g(|\xi^*-\xi|,\mu)\frac{\partial u_2^L}{\partial\xi}(\xi^*,\tau)\,\mathrm{d}\xi^*\right] +\bar{K}_L\left(\bar{u}_2^L-\bar{u}_1^L\right)\mathrm{H}(\bar{c}_1-\xi)+\bar{K}_L\left(\bar{u}_2^L-\bar{u}_1^R\right)(\mathrm{H}(\bar{c}_2-\xi)-\mathrm{H}(\bar{c}_1-\xi))=0;\ 0<x<\bar{c}_2, \tag{31c}$$

$$(1+\chi_1^2)\frac{\partial^2 u_2^R}{\partial\tau^2}-(1+\chi_2^2)\frac{\partial}{\partial\xi}\left[\int_{\bar{c}_2}^{1}\Gamma_0 g(|\xi^*-\xi|,\mu)\frac{\partial u_2^R}{\partial\xi}(\xi^*,\tau)\,\mathrm{d}\xi^*\right] +\bar{K}_L\left(\bar{u}_2^R-\bar{u}_1^R\right)=0;\ \bar{c}_2<\xi<1. \tag{31d}$$

Using Eq. (8), the given boundary conditions in Eqs. (29a)–(29d) can be rewritten in the dimensionless form as:

$$\bar{k}_1\left(\bar{u}_1^R(\bar{c}_1,\tau)-\bar{u}_1^L(\bar{c}_1,\tau)\right)=(1+\chi_2^2)\int_0^{\bar{c}_1}\Gamma_0 g(|\xi^*-\bar{c}_1|,\mu)\frac{\partial u_1^L}{\partial\xi}(\xi^*,\tau)\,\mathrm{d}\xi^*, \tag{32a}$$

$$\int_0^{\bar{c}_1} g(|\xi^*-\bar{c}_1|,\mu)\frac{\partial u_1^L}{\partial\xi}(\xi^*,\tau)\,\mathrm{d}x^* = \int_{\bar{c}_1}^{1} g(|\xi^*-\bar{c}_1|,\mu)\frac{\partial u_1^R}{\partial\xi}(\xi^*,\tau)\,\mathrm{d}x^*, \tag{32b}$$

$$\bar{k}_1\left(\bar{u}_2^R(\bar{c}_2,\tau)-\bar{u}_2^L(\bar{c}_1,\tau)\right)=(1+\chi_2^2)\int_0^{\bar{c}_2}\Gamma_0 g(|\xi^*-\bar{c}_2|,\mu)\frac{\partial u_2^L}{\partial\xi}(\xi^*,\tau)\,\mathrm{d}\xi^*, \tag{32c}$$

$$\int_0^{\bar{c}_2} g(|\xi^*-\bar{c}_2|,\mu)\frac{\partial u_2^L}{\partial\xi}(\xi^*,\tau)\,\mathrm{d}x^* = \int_{\bar{c}_1}^{1} g(|\xi^*-\bar{c}_2|,\mu)\frac{\partial u_2^R}{\partial\xi}(\xi^*,\tau)\,\mathrm{d}\xi^*. \tag{32d}$$

Eqs. (30a)-(30d) or (31a)–(31d) display four coupled integro-based equations of motion of the double nanorod system with local defects according to the nonlocal-integral-based elasticity theory of Eringen. To obtain free dynamic response of the nanosystem, these equations should be analyzed for the natural frequencies by satisfying the interfacial conditions given in (32a)–(32d) as well as the ends' conditions.

It should be noticed that the suggested nonlocal-integro-based model can be reduced to the classical one as the kernel function is replaced by the Kronecker delta function.

3.2. Frequency analysis using Galerkin method on the basis of admissible modes

In this part, evaluation of the natural frequencies of the defected nanosystem based on the proposed nonlocal-integral-surface energy-based model in the previous section is of concern. To this end, Galerkin approach in conjunction with admissible mode methodology is exploited. By following up the explained procedure in Section 2.2, we will arrive at a set of ordinary differential equations as that provided in Eq. (16). The nonzero-terms of the dimensionless mass and stiffness submatrices in the case of $\bar{c}_1 \geqslant \bar{c}_2$ are expressed as follows:

$$\overline{M}_{ij}^{(11)} = (1+\chi_1^2)\int_0^{\bar{c}_1}\varphi_i^{(1L)}\varphi_j^{(1L)}\mathrm{d}\xi, \tag{33a}$$

$$\overline{M}_{ij}^{(22)} = (1+\chi_1^2)\int_{\bar{c}_1}^{1}\varphi_i^{(1R)}\varphi_j^{(1R)}\mathrm{d}\xi, \tag{33b}$$

$$\overline{M}_{ij}^{(33)} = (1+\chi_1^2)\int_0^{\bar{c}_2}\varphi_i^{(2L)}\varphi_j^{(2L)}\mathrm{d}\xi, \tag{33c}$$

$$\overline{M}_{ij}^{(44)} = (1+\chi_1^2)\int_{\bar{c}_2}^{1}\varphi_i^{(2R)}\varphi_j^{(2R)}\mathrm{d}\xi, \tag{33d}$$

$$\overline{K}_{ij}^{(11)} = (1+\chi_2^2)\left(\lambda_j^{(1)}\right)^2\int_0^{\bar{c}_1}\int_0^{\bar{c}_1}\Gamma_0 g(|\xi^*-\xi|;\mu)\varphi_i^{(1L)}\varphi_j^{(1L)}\mathrm{d}\xi\mathrm{d}\xi^* +\bar{K}_L\int_0^{\bar{c}_1}\mathrm{H}(\bar{c}_1-\xi)\varphi_i^{(1L)}\varphi_j^{(1L)}\mathrm{d}\xi, \tag{33e}$$

$$\overline{K}_{ij}^{(13)} = -\bar{K}_L\int_0^{\bar{c}_1}\mathrm{H}(\bar{c}_2-\xi)\varphi_i^{(1L)}\varphi_j^{(2L)}\mathrm{d}\xi, \tag{33f}$$

$$\overline{K}_{ij}^{(14)} = -\bar{K}_L\int_0^{\bar{c}_1}(\mathrm{H}(\bar{c}_1-\xi)-\mathrm{H}(\bar{c}_2-\xi))\varphi_i^{(1L)}\varphi_j^{(2R)}\mathrm{d}\xi, \tag{33g}$$

$$\overline{K}_{ij}^{(22)} = (1+\chi_2^2)\left(\lambda_j^{(1)}\right)^2\int_{\bar{c}_1}^{1}\int_{\bar{c}_1}^{1}\Gamma_0 g(|\xi^*-\xi|;\mu)\varphi_i^{(1R)}\varphi_j^{(1R)}\mathrm{d}\xi\mathrm{d}\xi^*+\bar{K}_L\int_{\bar{c}_1}^{1}\varphi_i^{(1R)}\varphi_j^{(1R)}\mathrm{d}\xi, \tag{33h}$$

$$\overline{K}_{ij}^{(24)} = -\bar{K}_L\int_{\bar{c}_1}^{1}\varphi_i^{(1R)}\varphi_j^{(2R)}\mathrm{d}\xi, \tag{33i}$$

$$\overline{K}_{ij}^{(31)} = -\bar{K}_L\int_0^{\bar{c}_2}\varphi_i^{(2L)}\varphi_j^{(1L)}\mathrm{d}\xi, \tag{33j}$$

$$\overline{K}_{ij}^{(33)} = (1+\chi_2^2)\left(\lambda_j^{(1)}\right)^2\int_0^{\bar{c}_2}\int_{\bar{c}_1}^{1}\Gamma_0 g(|\xi^*-\xi|;\mu)\varphi_i^{(2L)}\varphi_j^{(2L)}\mathrm{d}\xi\mathrm{d}\xi^*+\bar{K}_L\int_0^{\bar{c}_2}\varphi_i^{(2L)}\varphi_j^{(2L)}\mathrm{d}\xi, \tag{33k}$$

$$\overline{K}_{ij}^{(41)} = -\bar{K}_L\int_{\bar{c}_2}^{1}(\mathrm{H}(\bar{c}_1-\xi)-\mathrm{H}(\bar{c}_2-\xi))\varphi_i^{(2R)}\varphi_j^{(1L)}\mathrm{d}\xi, \tag{33l}$$

$$\overline{K}_{ij}^{(42)} = -\bar{K}_L\int_{\bar{c}_2}^{1}(1-\mathrm{H}(\bar{c}_1-\xi))\varphi_i^{(2R)}\varphi_j^{(1R)}\mathrm{d}\xi, \tag{33m}$$

$$\overline{K}_{ij}^{(44)} = (1+\chi_2^2)\left(\lambda_j^{(1)}\right)^2\int_{\bar{c}_2}^{1}\int_{\bar{c}_2}^{1}\Gamma_0 g(|\xi^*-\xi|;\mu)\varphi_i^{(2R)}\varphi_j^{(2R)}\mathrm{d}\xi\mathrm{d}\xi^*+\bar{K}_L\int_{\bar{c}_2}^{1}\varphi_i^{(2R)}\varphi_j^{(2R)}\mathrm{d}\xi. \tag{33n}$$

Subsequently, by considering a harmonic form for the unknown coefficient vector, the dimensionless natural frequencies of the locally defected nanosystem according to the suggested nonlocal-integral-surface energy-based model are determined.

4. Results and discussion

Consider a nanosystem consists of doubly parallel silver nanorods with the following data [85,86]: $E_b = 76$ GPa, $\rho_b = 10{,}500$ kg/m^3, $\rho_0 = 10^{-7}$ kg/m^2, and $E_0 = 1.22$ N/m. In this part, we are interested in exploring the roles of the locations of the defects, defect factors, length, and diameter of the nanorod on natural frequencies of the defected-nanorod-system are explained and discussed in some detail. For each parametric study, the importance of nonlocality and surface energy effects on the obtained results is also highlighted. To this end, the predicted results based on the classical theory of elasticity (CTE), nonlocal-integral theory of elasticity theory (NTE), surface theory of elasticity (STE), nonlocal-integral-surface theory of elasticity (NSTE) are presented, and their results are compared with each other.

4.1. Some verification studies

In a special case, the predicted results by the suggested nonlocal-differential-based model are checked with those of Hsu et al. [80]. They investigated free longitudinal vibration of fixed-free and fixed–fixed individual nanorods accounting for only nonlocality (i.e., without considering the surface energy effect, $\chi_1 = \chi_2 = 0$). By ignoring the dynamical interactions between the constitutive nanorods of the nanosystem (i.e., $K_L = 0$), the predicted first six longitudinal frequencies by the proposed model and those of Hsu et al. [80] for both fixed-free and fixed–fixed boundary conditions have been given in Table 1. As it is seen, there exists a reasonably good agreement between the results of the present work and those of Hsu et al. [80].

In another comparison scrutiny, the capability of the proposed nonlocal-differential-based model in capturing free vibration of a defect-free nanosystem consists of double nanorods is going to be examined. To idealized the defect-free condition, we set $\bar{k}_1 = \bar{k}_2 = 10^5$ for a fixed-free nanosystem. The predicted fundamental frequencies of such a nanosystem in the lack of surface energy based on the suggested model by Murmu and Adhikari [60] and those of the present model are provided in Table 2. As it is seen, the present model can accurately predict the results of Ref. [60] with a good accuracy such that the relative error is lower than 0.5 percent for all considered values of the nonlocal parameter.

4.2. Nonlocal-integral model vs. nonlocal-differential model

In order to show the capabilities of the proposed nonlocal-differential-surface energy-based model (NDSM) in capturing the predicted vibration behavior of the defected nanosystem by the nonlocal-integral-surface energy-based model (NISM), their results are compared under various conditions. Tables 3 and 4 present the predicted first four natural frequencies of the fixed–fixed and fixed-free defected nanosystems. The unit of frequencies is THz, and these are provided for three lengths of nanorods (i.e., $l_b = 10$, 15, and 20 nm) and four defects' locations (i.e., $(\bar{c}_1, \bar{c}_2) = (0.6,0.5)$, $(0.7,0.6)$, $(0.8,0.7)$, and $(0.9,0.8)$) using the attenuating function $g(x; e_0a) = \exp\left(-\frac{|x|}{e_0a}\right)$. In the case of the fixed–fixed condition, by approaching the defects to the ends, the relative differences between the results by the NISM and those of the NDSM reduce; however, the variation of the nanorod length has a trivial effect on such differences. For fixed-free defected nanosystems, the predicted frequencies by the NDSM are closer to those obtained by the NISM comparing with fixed–fixed defected nanosystems. The presented results in Table 4 indicate that the maximum relative differences between the fundamental frequencies based on the NDSM and those of the NISM are lower than 6 percent for all considered levels of length and locations of defects.

4.3. Effect of the nonlocality

Fig. 2(a) displays the role of the small-scale parameter on the dominant frequencies of the fixed–fixed and fixed-free defected nanosystems for three levels of the defect factor (i.e., $\bar{k}_1 = \bar{k}_2 = 4$, 8, and 10,000). The plotted results show that the natural frequencies would reduce as the small-scale parameter increases, irrespective of the defect factor for both boundary conditions. This fact clearly indicates that the predicted longitudinal stiffness of the defected nanosystem based on the NTE is smaller than that obtained by the CTE. This could be interpreted by this reason that the diagonal elements of the mass matrices based on the NTE are commonly greater than those predicted by the CTE. It should be noted that we are employing a simple version of the nonlocal elasticity theory of Eringen in this work in which the nonlocality appears in the inertial terms as well as in the expressions of external force and external stiffness (i.e., attached springs and elastic layers). This issue is somewhat in contradiction with our sense regarding the nonlocality and small-scale effects. To remove this deficiency, appropriate nonlocal-integral models have been developed in recent years [17,78,79]. The application of these sophisticated versions of the NTE of Eringen to the problem at hand could be pursued by interested investigators. According to Fig. 2(a), as the defect factor increases, the nanosystem becomes stiffer, and the natural frequency would increase. Such a fact is more obvious in the absence of the nonlocality, particularly for frequencies of higher vibration modes.

Table 1
Verification of the predicted first six frequencies of an individual defected nanorod by the proposed model and those obtained by Hsu et al. [80] ($l_b = 20$ nm, $\bar{c}_1 = 4.004$ nm, $\bar{k}_1 = 8.7413$, $\chi_1 = \chi_2 = 0$).

		ω_i (THz)					
BCs°	Model	$i = 1$	$i = 2$	$i = 3$	$i = 4$	$i = 5$	$i = 6$
Fixed–fixed	Present work	2.9429	6.2236	9.3014	11.5213	14.5150	18.1342
	Hsu et al. [80]	2.9429	6.2236	9.3013	11.5211	14.5149	18.1339
Fixed-free	Present work	1.4278	4.5578	7.8540	10.4472	12.8743	16.2952
	Hsu et al. [80]	1.4278	4.5576	7.8540	10.4486	12.8741	16.2952

Table 2
Verification of the fundamental frequencies of a defect-free double-nanorod-system by Murmu and Adhikari [60] and those obtained by the proposed model for various small-scale parameters ($K_L = 8$ N/nm, $\bar{k}_1 = \bar{k}_2 = 10^5$).

	ω_1 (THz)			
Model	$e_0a = 0.5$ nm	$e_0a = 1$ nm	$e_0a = 1.5$ nm	$e_0a = 2$ nm
Ref. [60]	1.2353	0.8436	0.6137	0.4764
present work	1.2411	0.8477	0.6164	0.4782

Table 3
A comparison between the predicted first four frequencies of the defected fixed–fixed nanosystem based on the NDSM and those of the NISM ($\bar{k}_1 = \bar{k}_2 = 2$, $\overline{K}_L = 3$, $D_0 = 6$ nm, $e_0a = 1$ nm).

l_b	$\bar{c}_1 = 0.6$, $\bar{c}_2 = 0.5$		$\bar{c}_1 = 0.7$, $\bar{c}_2 = 0.6$		$\bar{c}_1 = 0.8$, $\bar{c}_2 = 0.7$		$\bar{c}_1 = 0.9$, $\bar{c}_2 = 0.8$	
(nm)	NDSM	NISM	NDSM	NISM	NDSM	NISM	NDSM	NISM
10	0.7975	0.9168	0.7549	0.8099	0.7046	0.7264	0.6606	0.6595
	1.0314	1.1450	1.0055	1.0461	0.9651	0.9766	0.9294	0.9253
	1.1956	2.1071	1.2817	1.8468	1.4124	1.6453	1.3617	1.4837
	1.3507	2.4440	1.4887	2.1059	1.5409	1.8616	1.5338	1.6782
15	0.5444	0.6253	0.5131	0.5517	0.4770	0.4943	0.4460	0.4484
	0.6977	0.7767	0.6781	0.7073	0.6488	0.6589	0.6234	0.6233
	0.8284	1.4386	0.8952	1.2561	1.0163	1.1160	0.9721	1.0043
	0.9311	1.6773	1.0555	1.4371	1.0970	1.2647	1.0899	1.1361
20	0.4118	0.4754	0.3875	0.4190	0.3597	0.3752	0.3360	0.3402
	0.5260	0.5886	0.5107	0.5350	0.4880	0.4977	0.4685	0.4704
	0.6299	1.0917	0.6827	0.9515	0.7848	0.8444	0.7482	0.7594
	0.7071	1.2767	0.8111	1.0904	0.8444	0.9575	0.8387	0.8589

Table 4
A comparison between the predicted first four frequencies of the defected fixed-free nanosystem based on the NDSM and those of the NISM ($\bar{k}_1 = \bar{k}_2 = 2$, $\overline{K}_L = 3$, $D_0 = 6$ nm, $e_0a = 1$ nm).

l_b	$\bar{c}_1 = 0.6$, $\bar{c}_2 = 0.5$		$\bar{c}_1 = 0.7$, $\bar{c}_2 = 0.6$		$\bar{c}_1 = 0.8$, $\bar{c}_2 = 0.7$		$\bar{c}_1 = 0.9$, $\bar{c}_2 = 0.8$	
(nm)	NDSM	NISM	NDSM	NISM	NDSM	NISM	NDSM	NISM
10	0.3501	0.3455	0.3689	0.3571	0.3889	0.3711	0.4065	0.3849
	0.7525	0.7484	0.7625	0.7559	0.7718	0.7626	0.7803	0.7680
	0.9581	0.9858	0.8999	0.9155	0.8912	0.8977	0.9488	0.9483
	1.1700	1.1892	1.1073	1.1131	1.0904	1.0900	1.1679	1.1661
15	0.2341	0.2357	0.2469	0.2435	0.2605	0.2529	0.2726	0.2622
	0.5018	0.5011	0.5087	0.5063	0.5153	0.5113	0.5212	0.5153
	0.6553	0.6702	0.6121	0.6213	0.6043	0.6084	0.6438	0.6424
	0.7953	0.8050	0.7477	0.7512	0.7341	0.7343	0.7907	0.7861
20	0.1758	0.1789	0.1854	0.1848	0.1957	0.1919	0.2049	0.1989
	0.3764	0.3767	0.3816	0.3807	0.3867	0.3846	0.3911	0.3878
	0.4959	0.5088	0.4623	0.4712	0.4559	0.4610	0.4858	0.4865
	0.6007	0.6096	0.5634	0.5678	0.5525	0.5542	0.5962	0.5934

To show the role of surface energy on the free vibration of the locally defected nanosystem, we perform another parametric study. In Fig. 2(b), the plots of the first three natural frequencies of the defected nanosystem as a function of the small-scale parameter have been demonstrated according to the NTE and NSTE. The predicted results by both the NTE and NSTE would lessen as the nonlocality becomes highlighted. In most of the cases, the results of the NSTE are greater than those of the NTE. This is basically related to the positive incorporation of the axial stiffness of the nanorod surface layer into the whole axial stiffness of the nanosystem. Furthermore, the impact of the surface energy on the fundamental frequency of the nanosystem is more apparent.

4.4. Effect of the defect location

The locations of both defects could seriously influence on the free vibration of the locally defected nanosystem. For this purpose, the plots of the fundamental frequencies of the defected nanosystem as a function of locations of the defects have been plotted in Fig. 3 for both fixed–fixed and fixed-free boundary conditions. It is observed that as the distance of the defects from the fixed ends increase, the fundamental frequency of the defected nanosystem would increase. Based on this fact, the maximum reduction of the longitudinal stiffness of the defected nanosystem would occur when the damages occur nearby the fixed supports. This fact holds true for both fixed–fixed and fixed-free conditions. In the case of fixed–fixed end condition, the plots of fundamental frequency in terms of the locations of the defects take its locally minimum points on the line $c_1 = c_2$. Actually, for a given value of c_2, the predicted nonlocal fundamental frequency of the defected nanosystem would grow with c_1 in the range of $c_1 \geqslant c_2$. This fact is more visible in the demonstrated results in Fig. 4.

In the lack of the surface energy effect, the plots of the fundamental frequency of the nanosystem as a function of the location of the local defect in the first nanorod have been provided in Fig. 4 for three levels of the small-scale parameter (i.e., $e_0a = 0$, 1, and 2 nm) in the case of $c_2 = 0.1$ nm. As it is seen, irrespective of the nonlocality level, the demonstrated graphs take their peak points at a certain level of c_1. The plotted results reveal that this level is not commonly affected by the nonlocal parameter. Additionally, for a considered value of c_1, the predicted fundamental frequencies of both fixed–fixed and fixed-free defected nanosystem generally reduce by growing of the nonlocal parameter. In the case of $c_1 = c_2$, the maximum influence of the nonlocality on the fundamental frequency is observed. In other words, the most impact of the nonlocality on the longitudinal stiffness of the nanosystem is observed when the nanosystem is defected at its fixed supports. Furthermore, the variation of the nonlocality has a less effect on the variation of the nanosystem stiffness when defects occur at the farthest places to the fixed ends.

In Fig. 5, for three levels of the location of the defect within the second nanorod (i.e., $c_2 = 1$, 3, and 5 nm for fixed–fixed condition and $c_2 = 3$, 5, and 8 nm for fixed-free condition), the variation of the fundamental frequency as a function of the defect location within the first nanorod has been plotted based on the CTE and NTE. The demonstrated results of the fixed–fixed defected nanosystem show that the maximum discrepancies between the predicted fundamental frequencies by the CTE and those of the NTE reach their maximum values when the defect of the second nanorod takes place at its midspan point. For various locations of the defect in the second nanorod, the

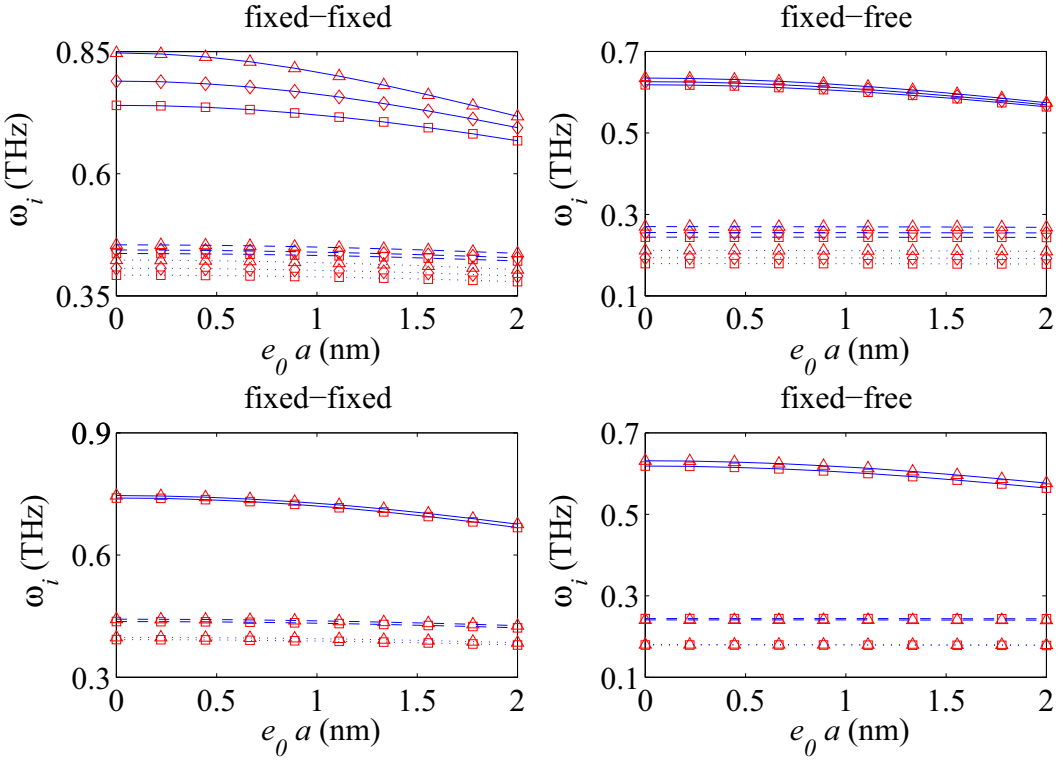

Fig. 2. The first three natural frequencies of the fixed–fixed and fixed-free defected nanosystems in terms of the small-scale parameter for: (a) different values of the defect parameter: ($\chi_1^2, \chi_2^2 = 0$; (□) $\bar{k}_1 = 4$, (◇) $\bar{k}_1 = 8$, (Δ)$\bar{k}_1 = 10000$, $\bar{K}_L = 0.7$), (b) both NTE- and NSTE-based models: ($l_b = 20$ nm, $D_0 = 0.5$ nm, $\bar{K}_L = 0.7$, $\bar{k}_1 = \bar{k}_2 = 4$; (□) NTE, (Δ) NSTE; $c_1 = 8$ nm, $c_2 = 5$ nm; (. . .) ω_1, (−−) ω_2, (—) ω_3).

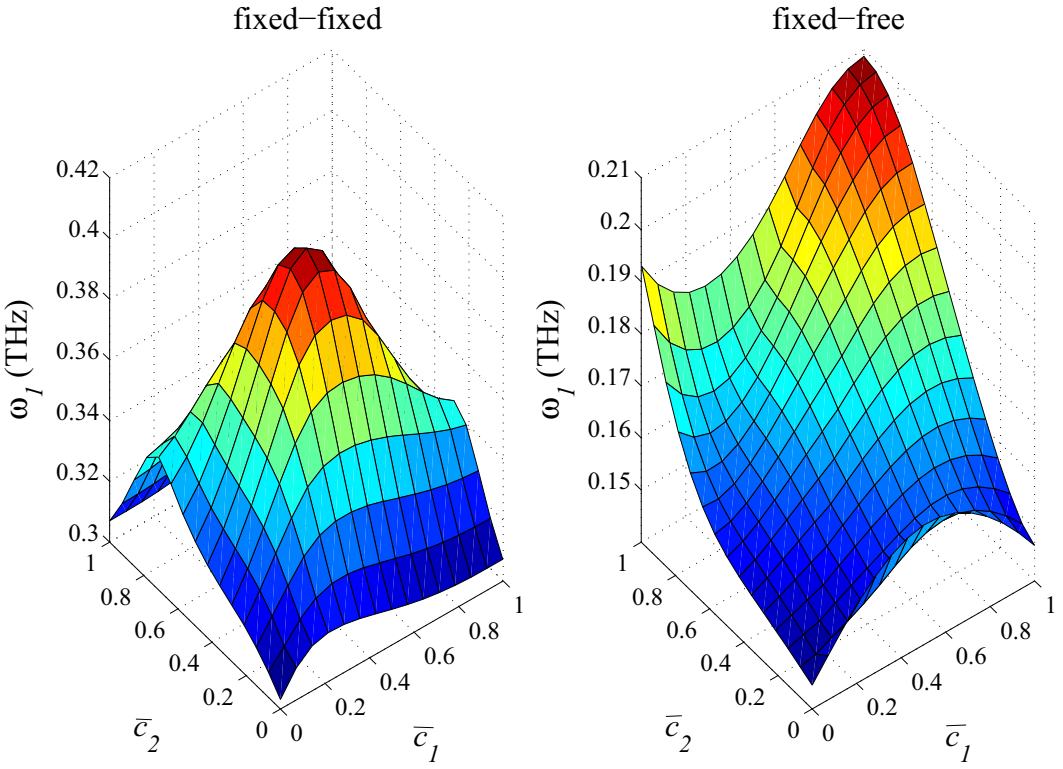

Fig. 3. The nonlocal fundamental frequencies of the fixed–fixed and fixed-free defected nanosystems in terms of the locations of the defects ($l_b = 20$ nm, $D_0 = 2$ nm, $\bar{k}_1 = \bar{k}_2 = 2$, $\bar{K}_L = 0.7$, $e_0 a = 2$ nm).

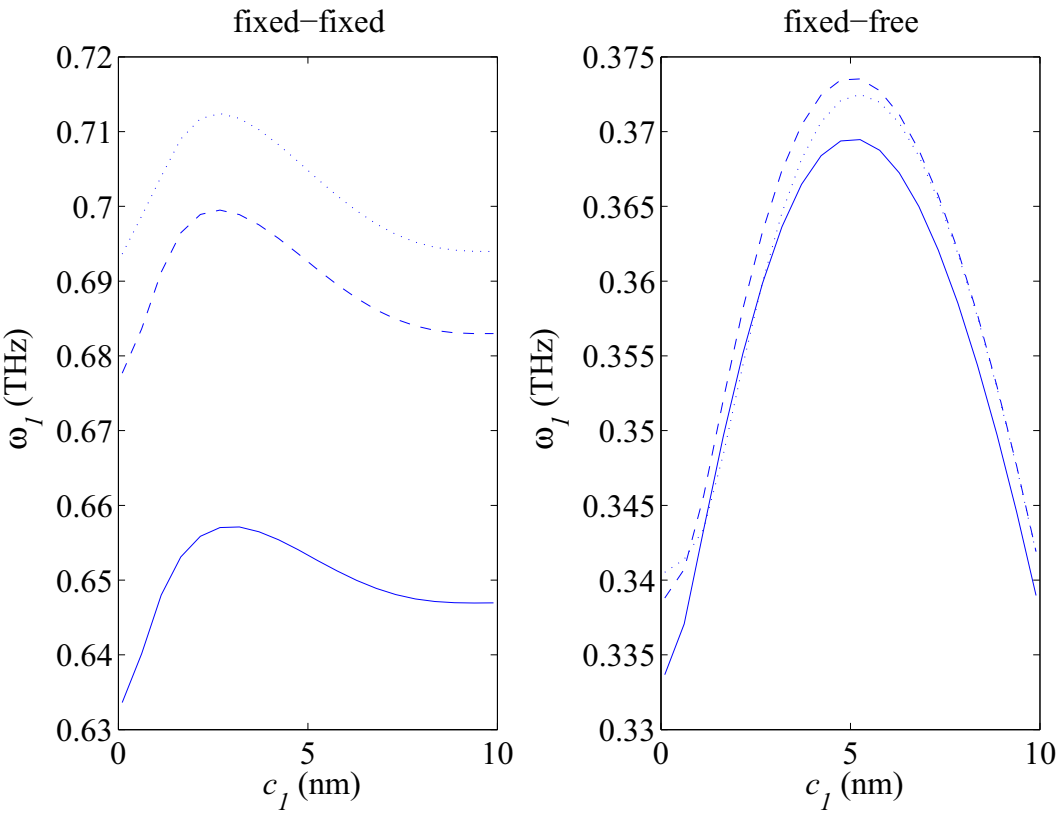

Fig. 4. The fundamental frequencies of the fixed–fixed and fixed-free defected nanosystems in terms of the defect location for various nonlocal parameters ($l_b = 10\,\text{nm}$, $D_0 = 0.5\,\text{nm}$, $c_2 = 0.1\,\text{nm}$; $(\ldots)$: (CTE : $e_0a = 0$); $(--)$: (NTE : $e_0a = 1$); (—):(NTE : $e_0a = 2\,\text{nm}$); $\bar{k}_1 = \bar{k}_2 = 4$, $\bar{K}_L = 0.7$).

minimum frequency of the fixed–fixed nanosystem is attained when the defect within the first nanorod occurs at its ends. In all studied cases, the maximum value of the fundamental frequency is observed for a particular arrangement of defects for the case that the first nanorod defect is placed just after the second nanorod defect. Concerning the fixed-free defected nanosystem, in the cases of $c_2 = 3$ and 5 nm, the occurrence of defect at the first nanorod support leads to the minimum possible frequency; however, in the case of $c_2 = 8$ nm, the longitudinal frequency reaches to its minimum level for the case of $c_1 \approx 2$ nm. Among various configurations of defects, the case of maximum frequency is associated with the nanosystem whose defects are placed close to the free ends.

4.5. Effect of the nanorod diameter

In Fig. 6(a), the variation of the fundamental frequency of the locally defected nanosystem in terms of the nanorod diameter has been plotted for fixed–fixed and fixed-free end conditions. The provided results are for three values of the small-scale parameter (i.e., $e_0a = 0$, 1, and 2 nm) in the case of $c_1 = c_2 = 8$ nm, $\bar{k} = 4$, and $\bar{K}_L = 0.7$. It is so obvious that the variation of the nanorod diameter has no influence on the variation of the fundamental frequency of the nanosystem based on the NTE. Actually, the NTE-based model could not capture the influence of the nanorod diameter on the fundamental frequency. In contrast to the NTE's results, the predicted results by the NSTE show that the fundamental frequency would commonly decrease by increasing the diameter. Factually, the ratio of the surface's strain energy to that of the bulk would increase by reducing the nanorod diameter. This fact is true for both fixed–fixed and fixed-free end conditions.

Fig. 6(b) displays the variation of the fundamental frequency of the defected nanosystem as a function of the nanorod diameter for five locations of the defects (i.e., $c_1 = c_2 = 2$, 4, 6, 8, and 10 nm). In most of the cases, the predicted results by the NSTE are greater than those of the NTE for both fixed–fixed and fixed-free conditions. Irrespective of the location of the occurred defects, the fundamental frequency by the NSTE would reduce by increasing the nanorod diameter and the results of the NSTE approach to those of the NTE. Both the NTE and the NSTE predict that the fundamental frequency of the defected nanosystem would increase as the defects become far away from the fixed ends. This issue is so apparent for both fixed–fixed and fixed-free end conditions. Additionally, the role of the surface energy on the fundamental frequency of nanosystems with defects furtherer to the fixed ends is more apparent.

4.6. Effect of the nanorod length

For various defect factors (i.e., $k_i^* = 0.01$, 1, and 100), the plots of the fundamental frequency of the defected nanosystem as a function of the nanorod length have been demonstrated in Fig. 7. The dimensionless defect factor and the interface constant have been defined such that the variation of the nanorod length has no influence on the variation of the defect factor as well as the interface constant. According to the demonstrated results for fixed–fixed and fixed-free boundary conditions, the fundamental frequency reduces by increasing the nanorod length. For the defected nanosystem with a higher defect factor, the variation of the nanorod length on the variation of the fundamental frequency is more influential, particularly in the case of the fixed-free boundary condition. In most cases, the predicted fundamental frequencies by the NSTE are greater than those obtained by the NTE. Furthermore, by increasing the nanorod length, the difference between

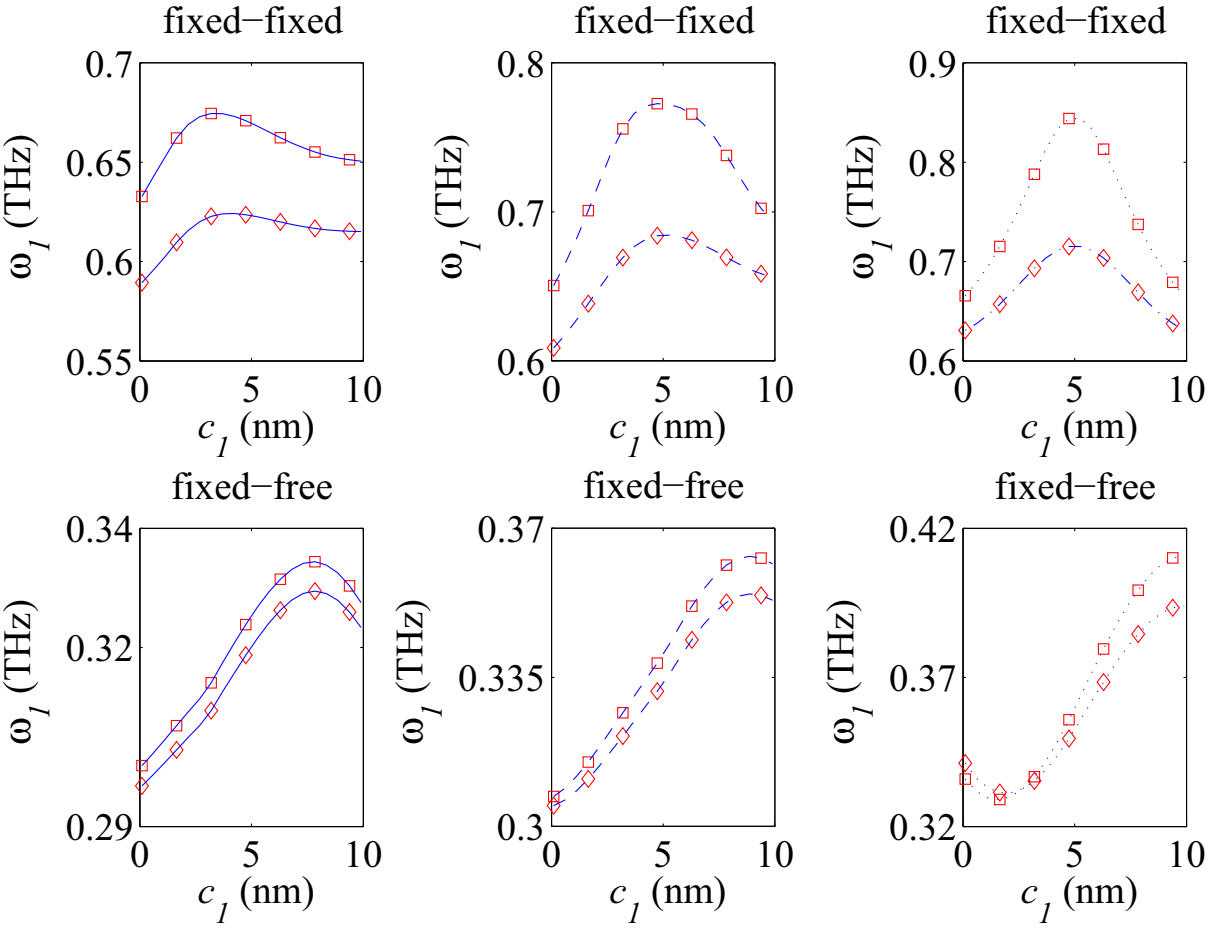

Fig. 5. The fundamental frequencies of the fixed–fixed and fixed-free defected nanosystems in terms of the locations of the defect in the first nanorod for various locations of the defect in the second nanorod (l_b = 10 nm, D_0 = 0.5 nm, $\bar{k}_1 = \bar{k}_2 = 2$, $\bar{K}_L$ = 0.7; ((—) c_2 = 1, (−−)c_2 = 3, (. . .)c_2 = 5 nm for fixed–fixed ends); ((—)c_2 = 3, (−−)c_2 = 5, (. . .)c_2 = 8 nm for fixed-free ends); (◇)NTE, (□) CTE; $\chi_1^2, \chi_2^2 = 0$).

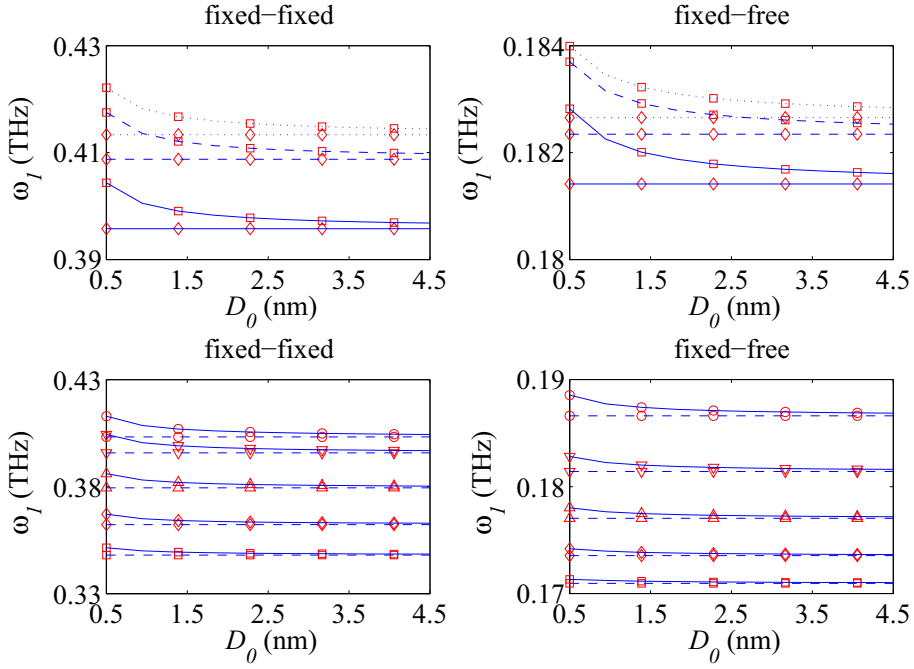

Fig. 6. The fundamental frequencies of the fixed–fixed and fixed-free defected nanosystems in terms of the nanorod diameter: (a) l_b = 20 nm, $c_1 = c_2$ = 8 nm, $\bar{k}_1 = \bar{k}_2 = 4$, $\bar{K}_L$ = 0.7, (. . .)e_0a = 0, (−−)e_0a = 1, (—) e_0a = 2 nm, (◇)NTE, (□)NSTE; (b) l_b = 20 nm, e_0a = 2 nm, $\bar{k}_1$ = 4, $\bar{K}_L$ = 0.7, (□)$c_1 = c_2$ = 2, (◇)$c_1 = c_2$ = 4, (Δ)$c_1 = c_2$ = 6, (∇)$c_1 = c_2$ = 8, (o)$c_1 = c_2$ = 10 nm, (−−) NTE, (—) NSTE.

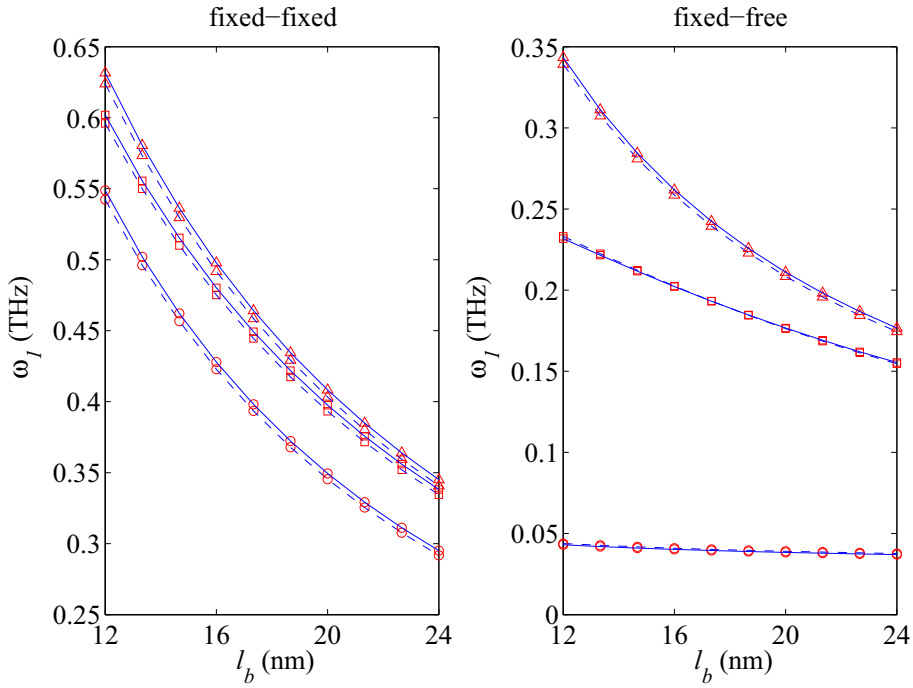

Fig. 7. The fundamental frequencies of the fixed–fixed and fixed-free defected nanosystems in terms of the nanorod length for different defect factors: $l_b = 20$ nm, $D_0 = 1$ nm, $e_0a = 2$ nm, $c_1 = 12$ nm, $c_2 = 8$ nm; (○) $\bar{k}_i^* = 0.01$, (□) $\bar{k}_i^* = 1$, (Δ) $\bar{k}_i^* = 100$, where $\bar{k}_i = \bar{k}_i^* \left(\frac{l_b}{l_b}\right)$, $\bar{K}_L = \bar{K}_L^* \left(\frac{l_b}{l_b}\right)^2$, $l_b^* = 12$ nm, $\bar{K}_L^* = 0.1$; (–) NTE, (—) NSTE.

these results magnify. This is mainly attributed to this issue that the ratio of the surface elastic energy to that of the bulk generally grows as the nanorod length increases.

5. Conclusions

Using novel nonlocal models, longitudinal vibrations of locally defected nanosystems consist of doubly adjacent nanorods were examined. By modeling the local defects via linear springs, each nanorod was subdivided into two separate parts. The dynamical interactions between the constituents of two nearby nanorods were visualized by a linear elastic layer. By employing the Hamilton's principle, the nonlocal-differential and the nonlocal-integral governing equations with their corresponding interfacial boundary conditions were displayed. Through evaluating the vibration modes that satisfy both interfacial and ends' conditions, we implemented the Galerkin approach based on the admissible modes to assess the free longitudinal vibration of the nanosystem. In a particular case, the results of the nonlocal-differential-based model were checked with those of another research work. The capabilities of the nonlocal-differential-surface energy-based model were also examined by comparing its results with those of the nonlocal-integral-surface energy-based model. The effects of nonlocality, surface energy, locations of the locally defected zones, mechanical properties of the defects, length and diameter of the nanorods on the dominant natural frequencies of the defected nanosystems were explained in some details.

The obtained results from this work plus to the exploited methodology for solving the equations of motion could be also employed for dynamical analysis of more generalized-defected nanosystems, particularly longitudinal vibrations of vertically aligned nanorods with multiple defects. Further, the main assumptions in the modeling of the problem were that the defects would be local and axisymmetric as well. The locality of defects allows us to ignore its size in comparison to the nanosystem length while the axisymmetric condition of the caused defects guarantee no interactions of the longitudinal modes with the transverse vibrational ones. Through violating the first condition, the defected zone would be no longer modeled by axial springs and the mixed actions of the damaged zones and the intact regions should be appropriately taken into account.

Declaration of Competing Interest

The authors declare that they have no known competing financial interests or personal relationships that could have appeared to influence the work reported in this paper.

Appendix A. Evaluation of the vibrational modes for the fixed–fixed and fixed-free defected nanorods

By neglecting the interactions between the constitutive nanorods, using Eqs. (9a) and (9b), the dimensionless equations of motion of the jth defected nanorod are stated as:

$$\left(1+\chi_1^2\right)\left(\frac{\partial^2 \bar{u}_j^L}{\partial \tau^2} - \mu^2 \frac{\partial^4 \bar{u}_j^L}{\partial \tau^2 \partial \xi^2}\right) - \left(1+\chi_2^2\right)\frac{\partial^2 \bar{u}_j^L}{\partial \xi^2} = 0;\ 0 < \xi < \bar{c}_j, \tag{A.1a}$$

$$\left(1+\chi_1^2\right)\left(\frac{\partial^2 \bar{u}_j^R}{\partial \tau^2} - \mu^2 \frac{\partial^4 \bar{u}_j^R}{\partial \tau^2 \partial \xi^2}\right) - \left(1+\chi_2^2\right)\frac{\partial^2 \bar{u}_j^R}{\partial \xi^2} = 0;\ \bar{c}_j < \xi < 1, \tag{A.1b}$$

with the following conditions at the defected zone (i.e., see Eqs. (11a) and (11b) at $\xi = \bar{c}_j$):

$$\bar{k}_j\left[\bar{u}_j^R(\bar{c}_j,\tau) - \bar{u}_j^L(\bar{c}_j,\tau)\right] = \left[\left(1+\chi_2^2\right) + \mu^2\left(1+\chi_1^2\right)\frac{\partial^2}{\partial \tau^2}\right]\frac{\partial \bar{u}_j^L}{\partial \xi}(\bar{c}_j,t), \tag{A.2a}$$

$$\left[\left(1+\chi_2^2\right) + \mu^2\left(1+\chi_1^2\right)\frac{\partial^2}{\partial \tau^2}\right]\frac{\partial \bar{u}_j^L}{\partial \xi}(\bar{c}_j,\tau) = \left[\left(1+\chi_2^2\right) + \mu^2\left(1+\chi_1^2\right)\frac{\partial^2}{\partial \tau^2}\right]\frac{\partial \bar{u}_j^R}{\partial \xi}(\bar{c}_j,\tau). \tag{A.2b}$$

By considering

$$\bar{u}_j^L(\xi,\tau) = \bar{U}_j^L(\xi)e^{i\varpi\tau};\ \bar{u}_j^R(\xi,\tau) = \bar{U}_j^R(\xi)e^{i\varpi\tau};\ i = \sqrt{-1}, \tag{A.3}$$

where $\bar{U}_j^L(\xi)$ and $\bar{U}_j^R(\xi)$ represent the dimensionless amplitudes field of the left segment and the right segment of the jth defect nanorod, respectively, and ϖ denotes its dimensionless longitudinal frequency. By introducing this form of displacements to Eqs. (A.1a) and (A.1b), one can arrive at:

$$\begin{pmatrix} 1 & 0 & 0 & 0 \\ 0 & 0 & \cos(\lambda) & \sin(\lambda) \\ \left(\bar{k}_j\cos(\lambda\bar{c}_j) - \varpi\sqrt{1+\chi_1^2}\right)\sqrt{\left(\begin{matrix}(1+\chi_2^2)-\\ \mu^2\varpi^2(1+\chi_1^2)\end{matrix}\right)}\sin(\lambda\bar{c}_j) & \left(\bar{k}_j\sin(\lambda\bar{c}) + \varpi\sqrt{1+\chi_1^2}\right)\sqrt{\left(\begin{matrix}(1+\chi_2^2)-\\ \mu^2\varpi^2(1+\chi_1^2)\end{matrix}\right)}\cos(\lambda\bar{c}_j) & -\bar{k}_j\cos(\lambda\bar{c}_j) & -\bar{k}_j\sin(\lambda\bar{c}_j) \\ -\lambda\sin(\lambda\bar{c}_j) & \lambda\cos(\lambda\bar{c}_j) & \lambda\sin(\lambda\bar{c}_j) & -\lambda\cos(\lambda\bar{c}_j) \end{pmatrix} \times \begin{pmatrix} A_1 \\ A_2 \\ B_1 \\ B_2 \end{pmatrix} = \begin{pmatrix} 0 \\ 0 \\ 0 \\ 0 \end{pmatrix}, \tag{A.8}$$

$$\frac{d^2\bar{U}_j^L}{d\xi^2} + \frac{(1+\chi_1^2)\varpi^2}{(1+\chi_2^2)-\mu^2\varpi^2(1+\chi_1^2)}\bar{U}_j^L = 0;\ 0 < \xi < \bar{c}_j, \tag{A.4a}$$

$$\frac{d^2\bar{U}_j^R}{d\xi^2} + \frac{(1+\chi_1^2)\varpi^2}{(1+\chi_2^2)-\mu^2\varpi^2(1+\chi_1^2)}\bar{U}_j^R = 0;\ \bar{c}_j < \xi < 1, \tag{A.4b}$$

with

$$\bar{k}_j\bar{U}_j^L(\bar{c}_j) + \left((1+\chi_2^2) - \mu^2\varpi^2(1+\chi_1^2)\right)\frac{d\bar{U}_j^L(\bar{c}_j)}{d\xi} = \bar{k}_j\bar{U}_j^R(\bar{c}_j), \tag{A.5a}$$

$$\frac{d\bar{U}_j^L(\bar{c}_j)}{d\xi} = \frac{d\bar{U}_j^R(\bar{c}_j)}{d\xi}, \tag{A.5b}$$

Eqs. (A.5a) and (A.5b) are second-order linear-homogeneous ordinary differential equations. In the case of $\varpi < \sqrt{\frac{(1+\chi_2^2)}{\mu^2(1+\chi_1^2)}}$, the general form of the displacements of the constitutive segments of the first defected nanorod is given by:

$$\bar{U}_j^L(\xi) = A_1\cos(\lambda\xi) + A_2\sin(\lambda\xi);\ 0 < \xi < \bar{c}_j, \tag{A.6a}$$

$$\bar{U}_j^R(\xi) = B_1\cos(\lambda\xi) + B_2\sin(\lambda\xi);\ \bar{c}_j < \xi < 1, \tag{A.6b}$$

where A_i and $B_i; i = 1$ and 2 are constants whose values and their relations are commonly determined by enforcing the end conditions, and $\lambda^2 = \frac{(1+\chi_1^2)\varpi^2}{(1+\chi_2^2)-\mu^2\varpi^2(1+\chi_1^2)}$. In the present work, the following boundary conditions are taken into account:

$$\text{Fixed} - \text{fixed}: \quad \bar{U}_j^L(0) = 0;\ \bar{U}_j^R(1) = 0, \tag{A.7a}$$

$$\text{Fixed} - \text{free}: \quad \bar{U}_j^L(0) = 0;\ \frac{d\bar{U}_j^R(1)}{d\xi} = 0. \tag{A.7b}$$

- *Fixed–fixed boundary condition*
  By introducing conditions in Eqs. (A.2a), (A.2b), and (A.7a) to Eqs. (A.6a) and (A.6b),

$$\begin{pmatrix} 1 & 0 & 0 & 0 \\ 0 & 0 & -\lambda sin(\lambda) & \lambda\cos(\lambda) \\ \left(\bar{k}_j\sin(\lambda\bar{c}_j) - \varpi\sqrt{1+\chi_1^2}\right)\sqrt{\left(\begin{matrix}(1+\chi_2^2)-\\ \mu^2\varpi^2(1+\chi_1^2)\end{matrix}\right)}\cos(\lambda\bar{c}_j) & \left(\bar{k}_j\sin(\lambda\bar{c}_j) + \varpi\sqrt{1+\chi_1^2}\right)\sqrt{\left(\begin{matrix}(1+\chi_2^2)-\\ \mu^2\varpi^2(1+\chi_1^2)\end{matrix}\right)}\cos(\lambda\bar{c}_j) & -\bar{k}_j\cos(\lambda\bar{c}_j) & -\bar{k}_j\sin(\lambda\bar{c}_j) \\ -\lambda\sin(\lambda\bar{c}_j) & \lambda\cos(\lambda\bar{c}_j) & \lambda\sin(\lambda\bar{c}_j) & -\lambda\cos(\lambda\bar{c}_j) \end{pmatrix} \times \begin{pmatrix} A_1 \\ A_2 \\ B_1 \\ B_2 \end{pmatrix} = \begin{pmatrix} 0 \\ 0 \\ 0 \\ 0 \end{pmatrix}, \tag{A.12}$$

and by setting the determinant of the coefficient matrix equal to zero, the characteristic equation is derived as follows:

$$2\bar{k}_j\sin\left(\sqrt{\frac{(1+\chi_1^2)\varpi^2}{(1+\chi_2^2)-\mu^2\varpi^2(1+\chi_1^2)}}\right) + \varpi\sqrt{1+\chi_1^2}\sqrt{(1+\chi_2^2)-\mu^2\varpi^2(1+\chi_1^2)}\times \left(\cos\left(\sqrt{\frac{(1+\chi_1^2)\varpi^2}{(1+\chi_2^2)-\mu^2\varpi^2(1+\chi_1^2)}}\right) + \cos\left((2\bar{c}_j-1)\sqrt{\frac{(1+\chi_1^2)\varpi^2}{(1+\chi_2^2)-\mu^2\varpi^2(1+\chi_1^2)}}\right)\right) = 0. \tag{A.9}$$

Through solving Eq. (A.9), infinite longitudinal frequencies of the jth defected nanorod in the dimensionless form are obtained (i.e., $\varpi_i^{(j)}$). By substituting these values into Eqs. (A.6a) and (A.6b), the ith vibrational modes of the fixed–fixed defected nanorods for the case of $A_2 = B_1 = 1$ take the following form:

$$\varphi_i^{(jL)}(\xi) = \sin\left(\lambda_i^{(j)}\xi\right);\ j = 1, 2, \tag{A.10a}$$

$$\varphi_i^{(jR)}(\xi) = \sin\left(\lambda_i^{(j)}\right)\cos\left(\lambda_i^{(j)}\xi\right) - \cos\left(\lambda_i^{(j)}\right)\sin\left(\lambda_i^{(j)}\xi\right), \tag{A.10b}$$

and the values of $\lambda_i^{(j)}$ are:

$$\lambda_i^{(j)} = \frac{\varpi_i^{(j)}\sqrt{1+\chi_1^2}}{\sqrt{(1+\chi_2^2)-\mu^2\left(\varpi_i^{(j)}\right)^2(1+\chi_1^2)}};\ i = 1, 2, \ldots, NM. \tag{A.11}$$

- *Fixed-free boundary condition*
  By imposing the boundary conditions in Eqs. (A.2a), (A.2b), and (A.7b), it is obtained:

and the if and only if condition for existence of non-trivial solution to Eq. (A.12) is that the determinant of the coefficient should be equal to zero. Therefore, the characteristic relation associated with fixed-free defected nanorod is displayed by:

$$\bar{k}_j \cos\left(\sqrt{\frac{\left(1+\chi_1^2\right)\varpi^2}{\left(1+\chi_2^2\right)-\mu^2\varpi^2\left(1+\chi_1^2\right)}}\right) - \varpi\sqrt{1+\chi_1^2}\sqrt{(1+\chi_2^2)-\mu^2\varpi^2(1+\chi_1^2)}\times \cos\left(\bar{c}_j\sqrt{\frac{\left(1+\chi_1^2\right)\varpi^2}{\left(1+\chi_2^2\right)-\mu^2\varpi^2\left(1+\chi_1^2\right)}}\right)\sin\left(\left(1-\bar{c}_j\right)\sqrt{\frac{\left(1+\chi_1^2\right)\varpi^2}{\left(1+\chi_2^2\right)-\mu^2\varpi^2\left(1+\chi_1^2\right)}}\right)=0. \tag{A.13}$$

By solving Eq. (A.13) for dimensionless longitudinal frequencies, their values are evaluated appropriately. For the ith frequency of the jth nanorod (i.e., ϖ_i^j), the corresponding longitudinal vibration modes of the fixed-free defected nanorods are readily calculated by using Eqs. (A.6a) and (A.6b) and setting $B_2 = A_1 = 1$:

$$\varphi_i^{(jL)}(\xi) = \sin\left(\lambda_i^{(j)}\xi\right), \tag{A.14a}$$

$$\varphi_i^{(jR)}(\xi) = \cos\left(\lambda_i^{(j)}\right)\cos\left(\lambda_i^{(j)}\xi\right) + \sin\left(\lambda_i^{(j)}\right)\sin\left(\lambda_i^{(j)}\xi\right). \tag{A.14b}$$

References

[1] Weintraub B, Chang S, Singamaneni S, Han WH, Choi YJ, Bae J, Kirkham M, Tsukruk VV, Deng Y. Density-controlled, solution-based growth of ZnO nanorod arrays via layer-by-layer polymer thin films for enhanced field emission. Nanotechnology 2008;19. 435302.

[2] Cunningham PD, Souza Jr JB, Fedin I, She C, Lee B, Talapin DV. Assessment of anisotropic semiconductor nanorod and nanoplatelet heterostructures with polarized emission for liquid crystal display technology. ACS Nano 2016;10:5769–81.

[3] Nabar BP, Butler ZC, Butler DP. Piezoelectric ZnO nanorod carpet as a NEMS vibrational energy harvester. Nano Energy 2014;10:71–82.

[4] Santra S, Luca AD, Bhaumik S, Ali SZ, Udrea F, Gardner JW, Ray SK, Guha PK. Dip pen nanolithography-deposited zinc oxide nanorods on a CMOS MEMS platform for ethanol sensing. RSC Adv 2015;5:47609–16.

[5] Kim HM, Cho YH, Lee H, Kim SI, Ryu SR, Kim DY, Kang TW, Chung KS. High-brightness light emitting diodes using dislocation-free indium gallium nitride/gallium nitride multiquantum-well nanorod arrays. Nano Lett 2004;4:1059–62.

[6] Willander M, Nur O, Zhao QX, Yang LL, Lorenz M, Cao BQ, Pérez JZ. Zinc oxide nanorod based photonic devices: recent progress in growth, light emitting diodes and lasers. Nanotechnology 2009;20. 332001.

[7] Wang X, Summers CJ, Wang ZL. Large-scale hexagonal-patterned growth of aligned ZnO nanorods for nano-optoelectronics and nanosensor arrays. Nano Lett 2004;4:423–6.

[8] Wang JX, Sun XW, Yang Y, Huang H, Lee YC, Tan OK, Vayssieres L. Hydrothermally grown oriented ZnO nanorod arrays for gas sensing applications. Nanotechnology 2006;1:4995.

[9] Eringen AC. Nonlocal polar elastic continua. Int J Eng Sci 1972;10(1):1–16.

[10] Eringen AC. Linear theory of nonlocal elasticity and dispersion of plane waves. Int J Eng Sci 1972;10(5):425–35.

[11] Eringen AC. On differential equations of nonlocal elasticity and solutions of screw dislocation and surface waves. J Appl Phys 1983;54:4703–10.

[12] Eringen AC. Nonlocal continuum field theories. Springer Science & Business Media; 2002.

[13] Li L, Hu Y, Li X. Longitudinal vibration of size-dependent rods via nonlocal strain gradient theory. Int J Mech Sci 2016;115:135–44.

[14] Canadija M, Barretta R, de Sciarra FM. A gradient elasticity model of Bernoulli-Euler nanobeams in non-isothermal environments. Euro J Mech A/Solids 2016;55:243–55.

[15] Numanoglu HM, Akgöz B, Civalek Ö. On dynamic analysis of nanorods. Int J Eng Sci 2018;130:33–50.

[16] Nazemnezhad R, Kamali K. An analytical study on the size dependent longitudinal vibration analysis of thick nanorods. Mater Res Exp 2018;5. 075016.

[17] Barretta R, Canadija M, Marotti de Sciarra F. Modified nonlocal strain gradient elasticity for nano-rods and application to carbon nanotubes. Appl Sci 2019. 9 (3):514.

[18] Karlicic DZ, Ayed S, Flaieh E. Nonlocal axial vibration of the multiple Bishop nanorod system. Math Mech Solids 2019;24(6):1668–91.

[19] Demir Ç, Civalek Ö. Torsional and longitudinal frequency and wave response of microtubules based on the nonlocal continuum and nonlocal discrete models. Appl Math Modell 2013;37(22):9355–67.

[20] Ebrahimi F, Barati MR. Magneto-electro-elastic buckling analysis of nonlocal curved nanobeams. Euro Phys J Plus 2016;131(9):346.

[21] Mercan K, Civalek Ö. Buckling analysis of Silicon carbide nanotubes (SiCNTs) with surface effect and nonlocal elasticity using the method of HDQ. Compos Part B-Eng 2017;114:34–45.

[22] de Sciarra FM. Finite element modelling of nonlocal beams. Physica E 2014;59:144–9.

[23] Challamel N, Zhang Z, Wang CM, Reddy JN, Wang Q, Michelitsch T, Collet B. On nonconservativeness of Eringe's nonlocal elasticity in beam mechanics: correction from a discrete-based approach. Arch Appl Mech 2014;84(9–11):1275–92.

[24] Demir Ç, Civalek Ö. A new nonlocal FEM via Hermitian cubic shape functions for thermal vibration of nano beams surrounded by an elastic matrix. Compos Struct 2017;168:872–84.

[25] Khaniki HB, Hosseini-Hashemi S. Dynamic transverse vibration characteristics of nonuniform nonlocal strain gradient beams using the generalized differential quadrature method. Euro Phys J Plus 2017;132(11):500.

[26] Civalek Ö, Demir Ç. A simple mathematical model of microtubules surrounded by an elastic matrix by nonlocal finite element method. Appl Math Comput 2016;289:335–52.

[27] Norouzzadeh A, Ansari R, Rouhi H. Nonlinear wave propagation analysis in Timoshenko nano-beams considering nonlocal and strain gradient effects. Meccanica 2018;53(13):3415–35.

[28] Thai S, Thai HT, Vo TP, Patel VI. A simple shear deformation theory for nonlocal beams. Compos Struct 2018;183:262–70.

[29] Barretta R, Faghidian SA, Luciano R, Medaglia CM, Penna R. Free vibrations of FG elastic Timoshenko nano-beams by strain gradient and stress-driven nonlocal models. Compos Part B-Eng 2018;154:20–32.

[30] Apuzzo A, Barretta R, Faghidian SA, Luciano R, de Sciarra FM. Free vibrations of elastic beams by modified nonlocal strain gradient theory. Int J Eng Sci 2018;133:99–108.

[31] Kiani K. Magnetically affected single-walled carbon nanotubes as nanosensors. Mech Res Commun 2014;60:33–9.

[32] Kiani K, Roshan M. Nonlocal dynamic response of double-nanotube-systems for delivery of lagged-inertial-nanoparticles. Int J Mech Sci 2019;152:576–95.

[33] Shariati A, Mohammad-Sedighi H, Zur KK, Habibi M, Safa M. On the vibrations and stability of moving viscoelastic axially functionally graded nanobeams. Materials 2020;13(7):1707.

[34] Jankowski P, Zur KK, Kim J, Reddy JN. On the bifurcation buckling and vibration of porous nanobeams. Compos Struct 2020;250. 112632.

[35] Civalek Ö, Uzun B, Yayli MO, Akgöz B. Size-dependent transverse and longitudinal vibrations of embedded carbon and silica carbide nanotubes by nonlocal finite element method. Eur Phys J Plus 2020;135:381.

[36] Ebrahimi F, Barati MR, Civalek Ö. Application of Chebyshev-Ritz method for static stability and vibration analysis of nonlocal microstructure–dependent nanostructures. Eng Comput 2019;36:953–64.

[37] Kiani K. Vibrations of biaxially tensioned-embedded nanoplates for nanoparticle delivery. Indian J Sci Technol 2013;6(7):4894–902.

[38] Phuc PV, Thai CH, Xuan HN, Wahab MA. Porosity-dependent nonlinear transient responses of functionally graded nanoplates using isogeometric analysis. Compos Part B-Eng 2019;164:215–25.

[39] Fan J, Rong D, Zhou Z, Xu C, Xu X. Exact solutions for forced vibration of completely free orthotropic rectangular nanoplates resting on viscoelastic foundation. Eur J Mech-A/Solids 2019;73:22–33.

[40] Ansari R, Torabi J, Norouzzadeh A. Bending analysis of embedded nanoplates based on the integral formulation of Eringen's nonlocal theory using the finite element method. Physica B 2018;534:90–7.

[41] Norouzzadeh A, Ansari R. Isogeometric vibration analysis of functionally graded nanoplates with the consideration of nonlocal and surface effects. Thin Walled Struct 2018;127:354–72.

[42] Zur KK, Arefi M, Kim J, Reddy JN. Free vibration and buckling analyses of magneto-electro-elastic FGM nanoplates based on nonlocal modified higher-order sinusoidal shear deformation theory. Compos Part B-Eng 2020;182. 107601.

[43] Fernández-Sáez J, Zaera R. Vibrations of Bernoulli-Euler beams using the two-phase nonlocal elasticity theory. Int J Eng Sci 2017;119:232–48.

[44] Barretta R, de Sciarra FM. Constitutive boundary conditions for nonlocal strain gradient elastic nano–beams. Int J Eng Sci 2018;130:187–98.

[45] Romano G, Barretta R, Diaco M, de Sciarra FM. Constitutive boundary conditions and paradoxes in nonlocal elastic nanobeams. Int J Mech Sci 2017;121:151–6.

[46] Barati MR. On wave propagation in nanoporous materials. Int J Eng Sci 2017;116:1–11.

[47] Barati MR, Zenkour A. A general bi-Helmholtz nonlocal strain-gradient elasticity for wave propagation in nanoporous graded double-nanobeam systems on elastic substrate. Compos Struct 2017;168:885–92.

[48] Karami B, Shahsavari D, Janghorban M, Li L. Wave dispersion of mounted graphene with initial stress. Thin Wall Struct 2018;122:102–11.

[49] Sahmani S, Aghdam MM. Nonlocal strain gradient beam model for postbuckling and associated vibrational response of lipid supramolecular protein micro/nano-tubules. Math Biosci 2018;295:24–35.

[50] Aydogdu M. Axial vibration of the nanorods with the nonlocal continuum rod model. Physica E 2009;41(5):861–4.

[51] Lim CW. Is a nanorod (or nanotube) with a lower Young's modulus stiffer? Is not Young's modulus a stiffness indicator?. Sci China Phys 2010;53(4):712–24.

[52] Narendar S, Gopalakrishnan S. Nonlocal scale effects on ultrasonic wave characteristics of nanorods. Physica E 2010;42(5):1601–4.

[53] Kiani K. Free longitudinal vibration of tapered nanowires in the context of nonlocal continuum theory via a perturbation technique. Physica E 2010;43 (1):387–97.

[54] Simsek M. Nonlocal effects in the free longitudinal vibration of axially functionally graded tapered nanorods. Comput Mater Sci 2012;61:257–65.

[55] Barretta R, de Sciarra FM, Diaco M. Small-scale effects in nanorods. Acta Mech 2014;225(7):1945–53.

[56] Aydogdu M, Elishakoff I. On the vibration of nanorods restrained by a linear spring in-span. Mech Res Commun 2014;57:90–6.
[57] Yayli MÖ. On the axial vibration of carbon nanotubes with different boundary conditions. Micro Nano Lett 2014;9:807–11.
[58] Apuzzo A, Barretta R, Fabbrocino F, Faghidian SA, Luciano R, de Sciarra FM. Axial and torsional free vibrations of elastic nano-beams by stress-driven two-phase elasticity. J Appl Comput Mech 2019;5(2):402–13.
[59] Barretta R, Canadija M, Luciano R, de Sciarra FM. Stress-driven modeling of nonlocal thermoelastic behavior of nanobeams. Int J Eng Sci 2018;126:53–67.
[60] Murmu T, Adhikari S. Nonlocal effects in the longitudinal vibration of double-nanorod systems. Physica E 2010;43(1):415–22.
[61] Narendar S, Gopalakrishnan S. Axial wave propagation in coupled nanorod system with nonlocal small scale effects. Compos Part B-Eng 2011;42(7):2013–23.
[62] Karlicic D, Cajic M, Murmu T, Adhikari S. Nonlocal longitudinal vibration of viscoelastic coupled double-nanorod systems. Euro J Mech-A/Solids 2015;49:183–96.
[63] Karlicic D, Cajic M, Murmu T, Kozic P, Adhikari S. Nonlocal effects on the longitudinal vibration of a complex multi-nanorod system subjected to the transverse magnetic field. Meccanica 2015;50(6):1605–21.
[64] Gurtin ME, Murdoch AI. A continuum theory of elastic material surfaces. Arch Ration Mech An 1975;57:291–323.
[65] Gurtin ME, Murdoch AI. Surface stress in solids. Int J Solids Struct 1978;14:431–40.
[66] Gurtin ME, Murdoch AI. Effect of surface stress on wave propagation in solids. J Appl Phys 1976;47:4414–21.
[67] Murdoch AI. The propagation of surface waves in bodies with material boundaries. J Mech Phys Solids 1976;24:137–46.
[68] Yan Z, Jiang LY. The vibrational and buckling behaviors of piezoelectric nanobeams with surface effects. Nanotechnology 2011;22. 245703.
[69] Hosseini-Hashemi S, Nazemnezhad R. An analytical study on the nonlinear free vibration of functionally graded nanobeams incorporating surface effects. Compos Part B-Eng 2013;52:199–206.
[70] Kiani K. Stability and vibrations of doubly parallel current–carrying nanowires immersed in a longitudinal magnetic field. Phys Lett A 2015;379 (4):348–60.
[71] Wang KF, Wang BL. A finite element model for the bending and vibration of nanoscale plates with surface effect. Finite Elem Anal Des 2013;74:22–9.
[72] Kiani K. In-plane vibration and instability of nanorotors made from functionally graded materials accounting for surface energy effect. Microsyst Technol 2017;23:4853–69.
[73] Hosseini M, Bahreman M, Jamalpoor A. Thermomechanical vibration analysis of FGM viscoelastic multi-nanoplate system incorporating the surface effects via nonlocal elasticity theory. Microsyst Technol 2017;23:3041–58.
[74] Attia MA, Mahmoud FF. Size-dependent behavior of viscoelastic nanoplates incorporating surface energy and microstructure effects. Int J Mech Sci 2017;123:117–32.
[75] Kiani K. Characteristics of shear horizontal waves in magnetically affected ultra-thin films accounting for surface effect. Wave Motion 2015;53:20–7.
[76] Kiani K. Propagation of in-plane shear waves in magnetically affected highly conductive nanofilms by considering both surface and nonlocality effects. J Vib Acoust 2016;138. 031001.
[77] Lu L, Guo X, Zhao J. On the mechanics of Kirchhoff and Mindlin plates incorporating surface energy. Int J Eng Sci 2018;124:24–40.
[78] Kiani K. Nonlocal-integro-differential modeling of vibration of elastically supported nanorods. Physica E 2016;83:151–63.
[79] Kiani K. Free dynamic analysis of functionally graded tapered nanorods via a newly developed nonlocal surface energy-based integro-differential model. Compos Struct 2016;139:151–66.
[80] Hsu JC, Lee HL, Chang WJ. Longitudinal vibration of cracked nanobeams using nonlocal elasticity theory. Curr Appl Phys 2011;11:1384–8.
[81] Yayli MÖ, Çerçevik AE. Axial vibration analysis of cracked nanorods with arbitrary boundary conditions. J Vibroeng 2015;17:2907–21.
[82] Loya J, López-Puente J, Zaera V, Fernández-Sáez J. Free transverse vibrations of cracked nanobeams using a nonlocal elasticity model. J Appl Phys 2009;105. 044309.
[83] Loya JA, Aranda-Ruiz JA, Fernández-Sáez J. Torsion of cracked nanorods using a nonlocal elasticity model. J Phys D Appl Phys 2014;47. 115304.
[84] Roostai H, Haghpanahi M. Vibration of nanobeams of different boundary conditions with multiple cracks based on nonlocal elasticity theory. Appl Math Model 2014;38:1159–69.
[85] Wang GF, Feng XQ. Timoshenko beam model for buckling and vibration of nanowires with surface effects. J Phys D Appl Phys 2009;42(15). 155411.
[86] He J, Lilley CM. Surface effect on the elastic behavior of static bending nanowires. Nano Lett 2008;8(7):1798–802.